IEEE Access
Multidisciplinary | Rapid Review | Open Access Journal

Date of publication xxxx 00, 0000, date of current version xxxx 00, 0000.
Digital Object Identifier 10.1109/ACCESS.2020.Doi Number

Improved-Fitness Dependent Optimizer Based FOI-PD Controller for Automatic Generation Control of Multi-Source Interconnected Power System in Deregulated Environment

AMIL DARAZ[1], SUHEEL ABDULLAH MALIK[1], HAZLIE MOKHLIS[2], (Senior Member, IEEE), IHSAN UL HAQ [1], FARHAN ZAFAR [1], NURULAFIQAH NADZIRAH MANSOR[2]

[1]Department of Electrical Engineering, Faculty of Engineering and Technology, International Islamic University, Islamabad 44000, Pakistan (e-mail: amil.phdee108@iiu.edu.pk; suheel.abdullah@iiu.edu.pk; ihsanulhaq@iiu.edu.pk; farhanzafar113@yahoo.com)
[2]Department of Electrical Engineering, Faculty of Engineering, University of Malaya, Kuala Lumpur, 50603, Malaysia (e-mail: hazli@um.edu.my; afiqah.mansor@um.edu.my)

Corresponding author: Amil Daraz (e-mail: amil.phdee108@iiu.edu.pk)

ABSTRACT This paper presents a Fractional Order Integral-Proportional Derivative (FOI-PD) controller for Automatic Generation Control (AGC) of two-area Interconnected Power System (IPS) with six multiple generations units in a restructured environment. Further, the two-area IPS is composed of multiple non-linearities with Time Delay (TD), Boiler Dynamic (BD), Governor Dead Zone/ Band (GDZ/ GDB) and Generation Rate Constraint (GRC). The gains of the proposed controller are optimized by a most recent powerful meta-heuristic algorithm known as Improved-Fitness Dependent Optimizer (I-FDO). The efficiency of the proposed approach is compared with other techniques such as Firefly Algorithm (FA), Fitness Dependent Optimizer (FDO) and Teaching Learning Based Optimization (TLBO) algorithms. Further, to enhance the performance of the system, Redox Flow Batteries (RFB) is incorporated in each area and Thyristor Controlled Series Compensator (TCSC) in the tie-line of the power system. Results reveal that our proposed approach performs superior in terms of less Overshoot (Os), Settling time (Ts) and Undershoot (Us). Robustness of the proposed controller is verified by changing system parameters within a range of ± (25) %.

INDEX TERMS Fractional Order Integral-Proportional Derivative (FOI-PD) controller, Deregulated Power System, Improved-Fitness Dependent Optimizer, Automatic Generation Control, Fractional Order Proportional Integral Derivative Controller (FOPID), and Load Frequency Control.

I. INTRODUCTION

The modern power system consists of complicated electrical networks with interconnected control areas. A reliable power system should be able to supply continuous power to support consumers demand at all time, considering load variations. Load variations in power system mainly affect the system's frequency and cause an imbalance between power generations and consumer utilization. On the other hand, the power system typically consists of active and reactive components; active power is accountable for constant frequency and whereas reactive power is responsible to maintain network voltage within tolerable limits. In this regard, AGC plays an important role to ensure stable power system operation and control during load variations. AGC is needed to maintain constant frequency within the acceptable range and tie-line power of interconnected area system [1- 3].

In the conventional power sector, Distribution Companies (DISCOs), Generation Companies (GENCOs) and Transmission Companies (TRANSCOs) are possessed by a single body known as Vertically Integrated Utility (VIU) which delivered power at the regulated tariff. However, development in power industries has changed the structure of VIU into deregulated power system in which GENCOs, TRANCOs and DISCOs are owned by separate entities and they function independently in the competitive electricity market. Each company has the authority to contract others in the same or different control areas [4, 5].

This article has been accepted for publication in a future issue of this journal, but has not been fully edited. Content may change prior to final publication. Citation information: DOI 10.1109/ACCESS.2020.3033983, IEEE Access

Regulations that govern all the electricity transactions and auxiliary services such as automatic generation control taken by the GENCOs and DISCOs are usually handled by a body known as Independent System Operator (ISO) [6, 7]. In this regard, several control approaches have been proposed previously by various researchers to control the system frequency and tie-line power of the interconnected system. The basic concept of DISCO Participation Matrix (DPM) in the restructured framework has been proposed in [8] by examining the bilateral conventions of the power system. Permar *et al.* in [9] have used an optimal feedback controller for the multi-generation unit in a deregulated system. Authors in [10] suggested AGC for three area IPS in the restructured environment and optimized the parameters of the controller by employing the Genetic Algorithm (GA). Debbarna *et al.* in [11] have suggested FOPID controller where the gains of the controller are tuned using Bacterial Foraging Optimization (BFO) approach for AGC of multi-area thermal reheat unit under restructured power system. Dellip Kamari *et al.* in [12] have used Tilt Integral Derivative (TID) controller for Load Frequency Control (LFC) of two area reheat, hydro and gas power unit under deregulated environment incorporated with GRC, GDB and Boiler Dynamic (BD). The gains of the proposed controller are tuned using hybridization of TLBO with pattern Search (PS) algorithm.

Authors in [13] have studied AGC of multi-source IPS considering Flexible Alternating Current Transmission System (FACTS) devices with DC/AC link in the restructured environment including GRC and GDB. Shiva *et al.* in [14] have proposed a PID controller for AGC of three area multi-unit deregulated system. Quasi Oppositional Harmony Search (QOHS) method have been used to optimize the gains of the proposed controller. However, in literature, the consequence of physical limitations such as GDZ, TD, GRC, and BD non-linearity is not observed which needs further inclusive study.

In literature, numerous researchers have focused on FACTS and energy storage devices for improved performance of power system dynamics and for damping out of frequency oscillation, respectively. Authors in [15] proposed Thyristor Controlled Phase Shifter (TCPS) for AGC of the hydrothermal unit under a deregulated environment. Padhan *et al.* in [16] described the impact of TCSC and Superconducting Magnetic Energy Storage (SMES) for enhancing the load frequency dynamics of IPS. A Capacitive Energy Storage (CES) device incorporated with Static Synchronous Series Compensator (SSSC) for the multi-generation unit under deregulated environment has been reported in [17]. Impact of SMES and Unified Power Flow Controller (UPFC) [18], RFB [19], RFB and UPFC [20], Interline Power Flow Controller (IPFC) and RFB [21, 22], and TCSC [23, 24] have also been considered for stabilizing the power frequency and dynamic performance of several test systems.

In the last few decades, meta-heuristic optimization algorithm has attained incredible attention in the field of engineering particularly for the optimization of power system problems. For example, these methods have been successfully employed for the optimization of controllers gain. In this aspect, authors in [25] have used Particle Swarm Optimization (PSO) for tuning of Fraction High Order Differential Feedback Controller (FHODFC) in LFC of IPS. Hasanien in [26] has used the PID controller tuned with Whale Optimization Algorithm (WOA) considering a new model of renewable energy sources and conventional power system with the inclusion of GRC and GDB non-linearities. Similarly, some other meta-heuristic techniques have also been used to study the AGC of interconnected power system such as Sine Cosine Algorithm (SCA) [27], Imperialist Competitive Algorithm (ICA) [28], Modified Group Search Optimization (MGSO) [29], Fitness Dependent Optimizer (FDO) [30], Improved Ant Colony Optimization (IACO) [31], Salp Swarm Algorithm (SWA) [32], PSO hybridized with Gravitational Search Algorithm (hPSO-GSA) [33], Improved Gray Wolf Optimization (IGWO) [34], and Volleyball Premier League (VPL) [35]. Therefore, it is worth to further study the application of meta-heuristic techniques to solve problems related to AGC. A literature review on a group of papers related to AGC studies is provided in Table 1. The table also comprises of system type i.e. conventional or deregulated, the number of areas, effects of non-linearity, structure of controllers, optimization techniques and generation source types considered in AGC problem.

The literature study recognizes that numerous control structure with various optimization methods has been used to solve the AGC problem of power systems. PID controller is widely used to solve the AGC problem due to its simple structure, easy operation and better performance. However, due to complexity and non-linear behaviour of power systems the fractional-order and fuzzy order controllers have been used to improve the performance of the system [36, 37]. Similarly, some other modified structures of controllers have been used for AGC problem such as Fractional -Order Fuzzy PID (FOFPID) [38], Fractional Order Integral (FOI) cascaded with FOPD controller [39]. Fuzzy Fractional-Order PI- Fractional-Order PD (FFOPI-FOPD) [40] and fuzzy PID with filter-based cascade controller i.e. FPIDF-(1 + PI) [41]. However, the literature divulges that no attempt has been made yet to develop FOI-PD controller which is the modified form of FOPID controller for solving multi-source interconnected power system under the deregulated environment. Therefore, in this study, the modified form of FOPID controller with I-FDO algorithm has been successfully applied for the AGC problem.

The performance of the AGC system can be improved by properly designing the controller and optimizing its parameter. Therefore, in this work, a novel modified FOPID controller called as FOI-PD controller is designed and developed for AGC of two areas, six-generation units under the deregulated environment with consideration of various non-linearities including TD, GDZ, BD and GRC.

This article has been accepted for publication in a future issue of this journal, but has not been fully edited. Content may change prior to final publication. Citation information: DOI 10.1109/ACCESS.2020.3033983, IEEE Access

A more recent, meta-heuristic algorithm called as Improved-Fitness Dependent Optimizer (I-FDO) is employed for the optimization of the proposed controller. Further, the dynamic profile of the system is enhanced by incorporating RFB in each area and TCSC in series with the tie-lines. The effectiveness of the proposed approach is compared with other algorithms such as FDO, FA and TLBO. Further, the proposed controller employing I-FDO technique is compared with other controllers such as FOPID, I-PD and PID controllers. Moreover, the robustness of the proposed controller is tested by changing the system parameters of the multi-source deregulated power system.

This paper is structured as follows; Section II describes the modelling of the system, followed by AGC in a deregulated power system and modelling of TCSC and RFB system. Section III discusses the controller's design and formulation of a fitness function. An overview of optimization algorithms followed by FDO and I-FDO algorithms are presented in section IV. Implementation of the proposed approach and results are described in Section V. Finally, some concluding comments are presented in sectionVI.

TABLE1. Breif literaure review of AGC.

Reference No	System Type	Generation Sources	Number of Areas	Non-Linearity Effect	Optimization Techniques	Controller Type	Other Device Used
[1]	Conventional	Thermal-Hydro	3	GRC, GDB	hIFA-PS	FPID	-
[2]	Conventional	Thermal-Hydro-PV	2	GRC, GDB, TD	ICA	FPIDN-FOI	-
[4]	Deregulated	Thermal	2	-	QOHS	PID	TCSC
[5]	Deregulated	Thermal	4	-	-	ANFIS	-
[6]	Deregulated	Thermal-Hydro	3	GRC, BD, GDB	2DOF-PIDN-FOID	ISA	DG, EV
[9]	Deregulated	Thermal-Hydro-Gas	2	-	Feedback controller	-	-
[10]	Deregulated	Thermal	3	-	PID	GA	-
[11]	Deregulated	Thermal	2	-	FOPID	BFOA	-
[12]	Deregulated	Thermal-Gas-Hydro-Solar	3	GRC, BD, GDB	TID	TLBO-PS	TCPS, SMES
[13]	Deregulated	Thermal-Gas-Hydro	2	GRC, GDB	PID	FA	
[14]	Deregulated	Thermal-Hydro	3	GRC, GDB	PI	QOHS	-
[15]	Conventional	Hydro-Thermal	2	GRC	I	PSO	TCPS
[16]	Conventional	Thermal-Thermal	2	GRC, TD	PID	DE	TCSC, SMES
[17]	Conventional	Thermal-Hydro-Gas	2	-	I	ICA	SSSC, CES
[18]	Deregulated	Thermal-Hydro-Gas	2	GRC, TD	Fuzzy-PID	FA	UPFC, SMES
[19]	Deregulated	Thermal-Hydro-Gas	2	GRC	AGC Regulators	-	RFB
[20]	Deregulated	Thermal-Hydro-Wind-Diesel	2	GRC, GDB, BD	MID	hDE-PS	UPFC, RFB
[21]	Deregulated	Thermal-Hydro	2	GRC, TD	I	BFOA	IPFC, RFB
[22]	Deregulated	Thermal-Thermal	2	GRC, TD	PIDF	DE	IPFC, RFB
[23]	Deregulated	Thermal-Gas-Hydro	2	GRC, GDB	I	IPSO	TCSC
[24]	Deregulated	Thermal-Thermal	2		I	GA	TCSC
[25]	Conventional	Thermal-Gas-Hydro	2	GRC, GDB	FHODFC	PSO	-
[26]	Conventional	Thermal-PV	2	-	PID	WOA	-
[27]	Conventional	Thermal- Geothermal-Solar	2	-	FOPID	SCA	-
[28]	Conventional	Thermal-Thermal-Thermal	3	GDB, TD	CFFOPI–FOPID	ICA	-
[29]	Deregulated	Thermal-Gas-Hydro	2	GRC, GDB	FO	IPSO-MGSO	SSSC
[30]	Conventional	Thermal-Gas-Hydro	2	GRC, GDB, TD, BD	I-PD, PID	FDO	-
[31]	Conventional	Thermal-Hydro	2	GDB	FPID	IACO	-
[32]	Conventional	Wind-Thermal-PV	2	GRC, TD, GDB	PID	SSA	
[33]	Conventional	Thermal-Gas-Hydro	2	GRC, GDB	PI-PD	PSO-GSA	-
[34]	Conventional	Wind, PV, Diesel	2	-	FO-T2-FPID	IGWO	BES, EV
[35]	Deregulated	Thermal- Hydro- Gas	2	GRC, GDB, BD	2-DOF-PI-FOPDN	VPL	
[45]	Deregulated	Thermal- Hydro-Gas-wind	3	GRC, GDB	PFMPID	GOA	RFB
Proposed Model	Deregulated	Thermal- Hydro-Gas-wind	2	GRC, GDB, TD, BD	FOI-PD	I-FDO	RFB, TCSC

II. SYSTEM MODELLING

A realistic model of two areas six-generation unit with several non-linearities of Boiler Dynamic (BD), Generation Rate Constraint (GRC), Time Delay (TD) and Governor Dead Zone (GDZ), in the restructured environment, is presented in Figure 5. Area-1 comprises of hydro, gas, thermal reheat, TCSC and RFB unit with two DISCOs (DISCO-1 and DISCO-2) and Area-2 consist of hydro, wind, thermal reheat and RFB unit with two DISCOs (DISCO-3 and DISCO-4). Thermal reheat generation unit composed of the turbine, governor and reheat with Transfer Function (TF) $\frac{1}{ST_1+1}$, $\frac{1}{ST_r+1}$ and $\frac{SK_1T_r+1}{ST_r+1}$ respectively. While gas power unit is composed of valve position TF ($\frac{1}{Sb_g+x_g}$), governor TF ($\frac{Sx_C+1}{Sy_C+1}$), fuel combustion reaction TF ($\frac{1}{ST_{cd}+1}$) and TF of compressor discharge ($\frac{ST_{cr}-1}{ST_f+1}$). TF of the hydro unit has consist of droop compensation ($\frac{ST_r+1}{ST_{rh}+1}$), governor ($\frac{1}{ST_{gh}+1}$) and penstock turbine ($\frac{-ST_w+1}{0.5ST_w+1}$).

This article has been accepted for publication in a future issue of this journal, but has not been fully edited. Content may change prior to final publication. Citation information: DOI 10.1109/ACCESS.2020.3033983, IEEE Access

Similarly, wind power system composed of hydraulic pitch actuator and turbine blade pitch with transfer function $\frac{(ST_{p1}+1)K_{p1}}{(1+S)(ST_{p2}+1)}$ and $\frac{K_{p2}}{(S+1)}$ respectively. Various non-linearities including GDZ, BD, TD and GRC have been incorporated in two area multi-generation IPS to make the realistic system. Generation rate constraint mainly affects the system performance due to the limitation of a turbine concerning power generation unit. The generation rate for thermal reheat system is around 3-10% p.u.MW/minute, while for the hydro system is 270%/minute for rising and 330%/minute for falling the generation. Governor dead band is the total quantity of speed changes where there is no change in valve position. The non-linear relationship of GDB is articulated as follows:

$$G(s) = 0.8 - S\frac{0.2}{\pi} \tag{1}$$

Where G(s) represents the transfer function of the Boiler Dynamic (BD) model integrated with reheat thermal unit for a steam generation under pressure. The block diagram of BD is depicted in Figure 1. Time delay (TD) may interrupt system stability if it is not addressed appropriately. In this study TD of 2 sec for AGC model has been considered. Each generation unit has its area participation factor (apf) and regulatory parameters that determine contribution in the nominal load. The sum of all apf in each area is equal to unity. Because of the presence of an enormous thermal unit, their participation factor is in the range of 50-60 %, and hydropower system is about 30%. Whereas, the generation of gas and wind power unit is lower and their participation factor is 10 to 15% respectively. In this work, the participation factor for hydro, thermal, and wind/ gas are assumed to be 0.3, 0.575 and 0.125 respectively.

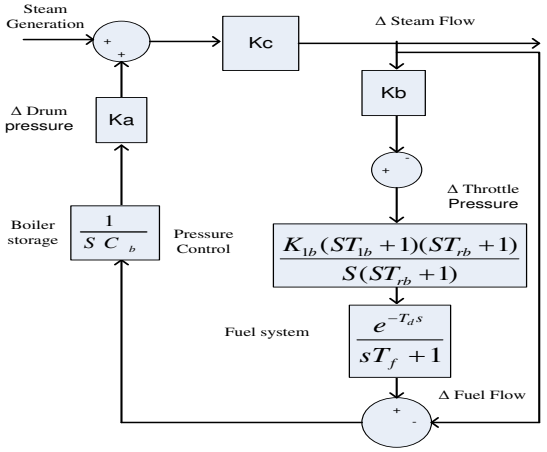

FIGURE 1. **Transfer function model of boiler.**

A. AGC in DEREGULATED POWER SYSTEM

In a deregulated system, GENCOs is permitted to trade power to any DISCO while a DISCO has the complete autonomy to deal with GENCOs in their area or any other area [4]. Such transaction is known as "bilateral transactions" which is supervised by ISO. The idea including DISCOs-GENCOs bilateral trading is articulated by DPM in which columns denote DISCOs and rows indicate GENCOs [8, 39]. Whereas, each entity in DPM shows Contract Participation Factor (cpf). Let us consider a two area IPS in a deregulated environment which is described by two DISCOs and three GENCOs in each control area and is expressed by (2) [20].

$$DPM = \begin{bmatrix} cpf_{11} & cpf_{12} & cpf_{13} & cpf_{14} \\ cpf_{21} & cpf_{22} & cpf_{23} & cpf_{24} \\ cpf_{31} & cpf_{32} & cpf_{33} & cpf_{34} \\ cpf_{41} & cpf_{42} & cpf_{43} & cpf_{44} \\ cpf_{51} & cpf_{52} & cpf_{53} & cpf_{54} \\ cpf_{61} & cpf_{62} & cpf_{63} & cpf_{64} \end{bmatrix} \tag{2}$$

In Eq (2) DPM represent DISCO Participation Matrix and cpf shows contract participation factor. Cpf signifies the fraction of each GENCOs contribution to the entire load demand of DISCOs. Whereas, diagonal elements denote the local demand and off-diagonal entities show the participation from other areas. The sum of all column elements of Eq (2) is equal to unity which can be expressed as below:

$$\sum_i cpf_{ij} = 1 \tag{3}$$

The scheduled tie line (ΔP_{tie12}^{Sch}) power may be expressed as

$$\Delta P_{tie12}^{Sch} = \sum_{m=1}^{2}\sum_{n=3}^{4} cpf_{mn}\Delta P_{Ln} - \sum_{m=3}^{4}\sum_{n=1}^{2} cpf_{mn}\Delta P_{Ln} \tag{4}$$

Where ΔP_{Ln} represents a change in DISCO load of n-th area. Error in tie-line power (ΔP_{tie12}^{Error}) from area-1 to area-2 is expressed as below:

$$\Delta P_{tie12}^{Error} = \Delta P_{tie12}^{actual} - \Delta P_{tie12}^{Sch} \tag{5}$$

Whereas

$$\Delta P_{tie12}^{actual} = \frac{2\Pi T_{12}}{s}\{\Delta f_1 - \Delta f_2\} \tag{6}$$

Where T_{12} shows synchronization constant of tie-line and Δf_1 , Δf_2 represents a change in the frequency of area-1 and area-2 respectively. Error in tie-line power (ΔP_{tie21}^{Error}) from area-2 to area-1 is expressed as follows:

$$\Delta P_{tie21}^{Error} = a_{12}\Delta p_{tie12}^{error} \therefore a_{12} = -1 \tag{7}$$

The Area Control Error (ACE) for area-1 and area-2 can be expressed as below:

$$ACE_1 = \beta_1\Delta f_1 + \Delta P_{tie12}^{Error} \tag{8}$$

$$ACE_2 = \beta_2\Delta f_2 + a_{12}\Delta P_{tie12}^{Error} \tag{9}$$

Where β_1 and β_2 represents the bias factor of area-1 and area-2 respectively.

B. TCSC MODELLING IN AGC

The flow of current for an interconnected area can be expressed as below:

$$I_{12} = \frac{|V_1|\angle\delta_1 - |V_2|\angle\delta_2}{J(X_{12} - X_{Tcsc})} \tag{10}$$

Where V_1, V_2, δ_1 and δ_2 represents terminal voltages and respective phase angles. Complex tie-line power can be articulated as:

$$P_{tie} - JQ_{tie12} = V_1^* I_{12} = |V_1|\angle(-\delta_1)\left[\frac{|V_1|\angle\delta_1 - |V_2|\angle\delta_1}{J(X_{12} - X_{Tcsc})}\right] \tag{11}$$

This article has been accepted for publication in a future issue of this journal, but has not been fully edited. Content may change prior to final publication. Citation information: DOI 10.1109/ACCESS.2020.3033983, IEEE Access

Where P and Q represent real and reactive power respectively. X_{Tcsc} shows reactance of TCSC and X_{12} represent reactance of tie-line. The real part of Eq (11) can be written as below:

$$P_{tie12} = \frac{|V_1|.|V_2|}{(X_{12} - X_{T\,csc})}[Sin(\delta_1 - \delta_2)] \quad (12)$$

The above equation in respect of percentage compensation (K_c) can be expressed as

$$P_{tie12} = \frac{|V_1|.|V_2|}{X_{12}(1 - K_c)}[Sin(\delta_1 - \delta_2)] \quad (13)$$

Where K_c denote degree of compensation and can be written as:

$$K_c = \frac{X_{T\,csc}}{X_{12}} \quad (14)$$

Equation (13) can be written as

$$P_{tie12} = \frac{|V_1|.|V_2|}{(X_{12} - X_{T\,csc})}[Sin(\delta_1 - \delta_2] + \frac{K_c}{(1 - K_c)}\frac{|V_1|.|V_2|}{(X_{12})}[Sin(\delta_1 - \delta_2] \quad (15)$$

The first term in Eq (15) represents tie-line power without TCSC while the second term denotes tie-line power with TCSC. The incremental tie-line power can be attained as:

$$\Delta P_{tie12} = \frac{|V_1|.|V_2|}{(X_{12})}[\cos(\delta_1^{\circ} - \delta_2^{\circ})][Sin(\Delta\delta_1 - \Delta\delta_2)] + \frac{\Delta K_c}{(1 - \Delta K_c)}\frac{|V_1|.|V_2|}{(X_{12})}[Sin(\delta_1^{\circ} - \delta_2^{\circ}] \quad (16)$$

Since the deviation of the bus voltage angle is practically small for minor variation in the actual power load, therefore, $Sin(\Delta\delta_1 - \Delta\delta_2) \approx \Delta\delta_1 - \Delta\delta_2$ (17)

$$\Delta P_{tie12} = \frac{|V_1|.|V_2|}{(X_{12})}[\cos(\delta_1^{\circ} - \delta_2^{\circ})][(\Delta\delta_1 - \Delta\delta_2)] + \frac{\Delta K_c}{(1 - \Delta K_c)}\frac{|V_1|.|V_2|}{(X_{12})}[Sin(\delta_1^{\circ} - \delta_2^{\circ}] \quad (18)$$

Let us consider

$$T_{12} = \frac{|V_1|.|V_2|}{(X_{12})}[\cos(\delta_1^{\circ} - \delta_2^{\circ})] \text{ and } K_{12} = \frac{|V_1|.|V_2|}{(X_{12})}[Sin(\delta_1^{\circ} - \delta_2^{\circ}] \quad (19)$$

$$\Delta P_{tie12} = [T_{12}(\Delta\delta_1 - \Delta\delta_2)] + \frac{\Delta K_c}{(1 - \Delta K_c)}[K_{12}] \quad (20)$$

Hence

$$\Delta\delta_1 = 2\Pi\int \Delta f_1 dt \quad (21)$$

$$\Delta\delta_2 = 2\Pi\int \Delta f_2 dt \quad (22)$$

By substituting values of Eq (21) and (22) into Eq (20) and also taking Laplace Transform, Eq. (20) can be written as:

$$\Delta P_{tie12}(s) = \frac{2\Pi T_{12}}{S}[\Delta f_1(s) - \Delta f_2(s)] + \frac{\Delta K_c}{(1 - \Delta K_c)}[K_{12}] \quad (23)$$

In Eq (23) the tie-line power can be controlled by ΔK_c and can be written as:

$$K_c = \frac{K_{T\,csc}}{1 + ST_{T\,csc}} \quad (24)$$

Where K_{Tcsc} and T_{Tcsc} represent gain and time constant of TCSC. If the input signal to the TCSC damping controller is assumed to be the change in error and TF of the signal conditioning circuit as:

$$\Delta K_c(s) = \frac{K_{T\,csc}}{1 + ST_{T\,csc}}[\Delta Error(s)] \quad (25)$$

$$\Delta K_c(s) = \frac{K_{T\,csc}}{1 + ST_{T\,csc}}[\Delta f_1(s)] \quad (26)$$

C. RFB MODELLING IN AGC

Redox flow batteries (RFBs) are made of electrolytes containing the active redox species contained in external tanks. Usually, cells are organised in bipolar stacks, in which the electrolytes flow during charge and discharge. Subsequently, the storage capacity is then calculated with respect to electrolyte tank size and the reactant concentraton, while the energy is determined by the number, configuration and choice of component of cell stacks. The soluable flow batteries gained attention over other devices to work efficiently without a cell separation membrane. RFBs are power devices which can be used as a frequency fluctuations stabilizer besides a fast energy compensation source. RFB can be considered as an energy storage device to reduce fluctuation in frequency and tie-line power of an IPS [21, 22, 39]. RFB is used more frequently as compared to other storage devices like SMES owing to its simple operation under normal temperature, low losses and long lifespan and maintenance. During abrupt changes in load, the RFB device delivers energy to the system and also charged constantly during system operation. RFB model of the system output versus frequency variation is expressed as follows:

$$\Delta P_{RFB} = \frac{K_{RFB}}{1 + T_{RFB}}[\Delta f] \quad (27)$$

Where T_{RFB} shows time constant and K_{RFB} denote gain of RFBs.

III. CONTROLLERS DESIGN AND FITNESS FUNCTION

Various controllers have been designed and implemented for AGC in literature. However, fractional-order controller attained considerable attention in the last few decays as compared to traditional controllers due to better disturbance rejection ratio, low noise effect and reduction of calculation time [28, 42]. In this section, a modified FOPID controller known as FOI-PD controller is designed and developed for AGC problem in a deregulated environment. The structure of FOPID and FOI-PD controllers are shown in Figure 2 and 3 respectively, which consist of five parameters, integral gain (K_i), derivative gain (K_d), proportional gain (K_p), fractional integrator order (λ) and fractional derivative order (μ). In FOPID controller all the parameters are put in feedforward direction while, in FOI-PD controller, the integral parameter (K_i) with integrator order (λ) is put in a forward direction and the remaining parameters are put in feedback [43]. The output of FOPID and FOI-PD controllers in terms of a differential equation is specified by Eq (28) and Eq (29) respectively.

$$u(t) = k_p e(t) + K_i D^{-\lambda} e(t) + K_d D^{\mu} e(t) \quad (28)$$

$$u(t) = K_i D^{-\lambda} e(t) - [k_p y(t) + K_d D^{\mu} y(t)] \quad (29)$$

Where u(t) represent control signal, e(t) denotes error signal, which is ACE in this case and y(t) is the output of the system. A step-change in the reference input R(s) of the FOPID controller will cause an instant spike change in the output of control signal U(s). This spike in the controller output is called as proportional or derivative kick which effects rapidly change the command signal to the actuator and can cause a serious problem in the plant G_p (s). To

This article has been accepted for publication in a future issue of this journal, but has not been fully edited. Content may change prior to final publication. Citation information: DOI 10.1109/ACCESS.2020.3033983, IEEE Access

overcome these drawbacks the modified structure of FOPID controller is introduced. In this structure, the integral gain responds on error signal E (s). An instant change in the reference input will not affect the derivative and proportional gains, since these two gains work on the output process Y(s) [44, 45].

The Transfer Function (TF) of the closed-loop system by considering a plant $G_p(s)$ with FOPID and FOI-PD controllers are given by Eq (29) and (30) respectively.

$$\frac{Y(s)}{R(s)} = \frac{G_p(s)[K_p S^{\lambda} + K_i + S^{\lambda} K_d S^{\mu}]}{S^{\lambda} + G_p(s)[K_p S^{\lambda} + K_i + S^{\lambda} K_d S^{\mu}]} \tag{30}$$

$$\frac{Y(s)}{R(s)} = \frac{G_p(s) K_i}{S^{\lambda} + G_p(s) K_i + K_p S^{\lambda} + S^{\mu} K_d S^{\lambda}} \tag{31}$$

Eq (30) shows that there are two zeros with FOPID controller which is tough to adjust the response of the system with these zeros. Their impact takes place as higher overshoot or an earlier peak. The proposed modified FOPID controller known as FOI-PD controller gets over these effect of zeros as shown in Eq (31) and enhances the response of the system by adding derivative and proportional terms of FOPID on feedback path instead of feedforward. Therefore, the response of the system with FOI-PD controller is achieved better as compared to FOPID controller which will be evident in the section of results and discussion.

To evaluate the performance of the proposed I-FDO method, Integral of Time-weighted Squared Error (ITSE) [23, 29, 30 and 45] is used as cost function to optimize AGC problem. ITSE expression can be written as:

$$J_1 = ITSE = \int_0^t \left[\Delta f_1^2 + \Delta f_2^2 + \Delta P^2_{tie12}\right] t dt \tag{32}$$

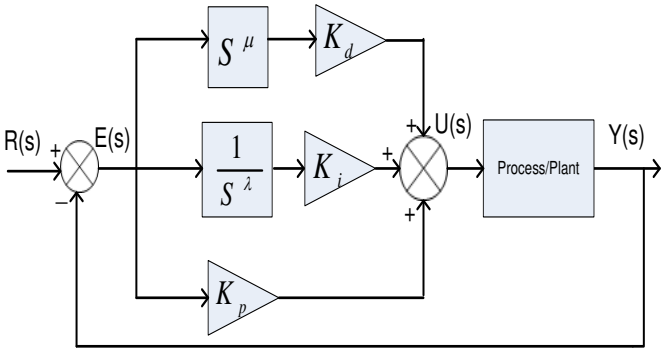

FIGURE 2. **Structure of FOPID controller.**

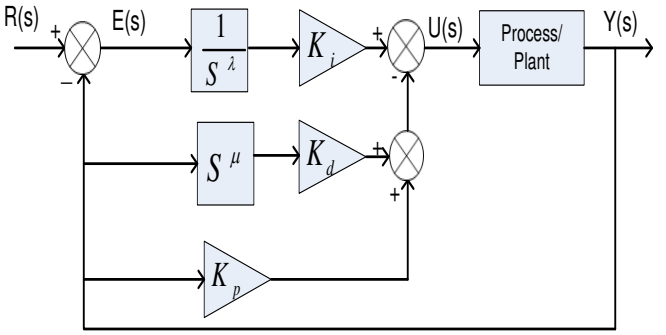

FIGURE 3. **Structure of FOI-PD controller.**

IV. OPTIMIZATION TECHNIQUES

A. FITNESS DEPENDENT OPTIMIZER (FDO)

In recent years, researchers are trying to develop a new meta-heuristic algorithm for optimization problems. In this aspect, Abdullah and Tarik developed a new algorithm in 2019 that is inspired by nature-based bee swarming reproductive process. This algorithm has been tested on 19 classical benchmark functions and three practical problems which shows outstanding performance as compared to other recent techniques [46]. Furthermore, the efficiency of the algorithm has also been evaluated on AGC problem [30] and also for the optimization of one-dimensional bin packing combinatorial problem [47]. FDO algorithm has fewer parameters comparing to other algorithms, this makes FDO much simpler, less complex, and faster. FDO algorithm consists of the following four steps:

1) STEP 1 (INITIALIZATION of POPULATION)

In this step, a population of scout bee in search space X_k (1, 2 …n) is initialized randomly. The number of the scout bees were equal to population size and each scout contains five parameters known as K_i, K_p, K_d, λ and μ denotes the gains of FOI-PD/FOPID controllers. Where each scout signifies the potential of solution and is trying to search a better hive (solution) by probing more positions randomly.

2) STEP 2 (FITNESS WEIGHT of SCOUT BEE)

Fitness weight (F_w) of the scout bee can be evaluated as:

$$F_w = \left|\frac{f(X^*_{k,t})}{f(X^t_k)}\right| - \gamma \tag{33}$$

Where $f(X^t_k)$ denotes the current value of fitness at iteration (t), $f(X^*_{k,t})$ represents fitness value for the global best solution and γ represents weight factor and its value is either 1 or 0. In most cases, its value is 0 for a stable search. However, this value also depends on a case by case problem.

3) STEP 3 (MOVEMENT of SCOUT BEE)

The movement of scout bee from their current position to a next position by adding pace *(P)* to explore better position can be expressed as follows:

$$X^{t+1}_k = X^t_k + P \tag{34}$$

Where X^{t+1}_k represents the next position, X^t_k denotes the current position and *P* represents the moment of scout bees. Pace (*P*) depends on F_w for a different case as given in Eq (35) and also its direction is based on random phenomena.

$$P = \begin{cases} \gamma(X^t_k - X^*_{k,t}) - 1; \text{If } 0<\gamma<1 \text{ and } \Gamma<0 \\ \gamma(X^t_k - X^*_{k,t}); \text{If } 0<\gamma<1 \text{ and } \Gamma \geq 0 \\ \Gamma X^t_i; \text{If } \gamma = 1 \text{ or } \gamma = 0 \text{ or } f(X^t_i) = 0 \end{cases} \tag{35}$$

Where Γ belongs to random values in the range of [-1, 1].

4) STEP 4 (STOPPAGE CRITERIA)

The fitness value of each scout bee is calculated until a solution is achieved or a termination criterion is reached.

This article has been accepted for publication in a future issue of this journal, but has not been fully edited. Content may change prior to final publication. Citation information: DOI 10.1109/ACCESS.2020.3033983, IEEE Access

B. IMPROVED- FITNESS DEPENDENT OPTIMIZER (I-FDO)

I-FDO is the improved form of FDO which was recently developed by Danieal *et al.* [48] and has been tested on 19 classical benchmark functions and shows its superiority from FDO and other recent metaheuristic algorithms. The concept of algorithm is based on the collective decision-making and generative process used by bees. Our proposed I-FDO algorithm differs from FDO algorithms which consist of two phases including position updates of scout bees and randomization of weight factor (γ).

1) UPDATING THE SOUT BEE POSITION

In I-FDO algorithm, the position of the scout's bee is updated by adding two parameters that are Alignment (A) and Cohesion (C) to original FDO. These two parameters are important signifiers of group motion; alignment (A) which shows pace matching of individuals in the neighbourhood or group to that of other individuals whereas, cohesion (C) is the tendency of scouts towards the centre of mass of the neighbourhood. The new position of artificial scout's bee can be articulated as follows:

$$X_k^{t+1} = X_k^t + P + (A \times \frac{1}{C}) \tag{36}$$

Where X_k^{t+1} represents the next position, X_k^t denotes the current position, P represents the moment of scout bees, A represent alignment and C represents the cohesion of scouts bee. Whereas alignment and cohesion are expressed in Eq (37) and (38) respectively.

$$A_i = \sum_{i=1}^{N} \frac{P_i}{N} \tag{37}$$

$$A_i = \sum_{i=1}^{N} \frac{X_i}{N} - X \tag{38}$$

Where P_i represents the pace of i-th neighbouring scouts bee, N represents the neighbourhood number, X is the position of current individuals and X_i is the position of i-th neighbouring scout.

2) RANDOMIZATION of WEIGHT FACTOR

In I-FDO algorithm weight factor (γ) is generated in the range of [0, 1] by using random phenomenon to control the fitness weight (F_W) instead of original FDO in which weight factor is considered to be 0 or 1. However in FDO, for most cases, the weight factor is used to be 0. In I-FDO algorithm improvement in terms of fitness weight can be written as below:

$$F_w = \left| \frac{f(X_{k,t}^*)}{f(X_k^t)} \right| \tag{39}$$

In Eq (39) if the value of Fitness weight (F_W) is equal to or less than generated weight factor (γ) then weight factor can be ignored otherwise, compared to the previous one.

The flow chart for I-FDO algorithm is depicted in Figure 4.

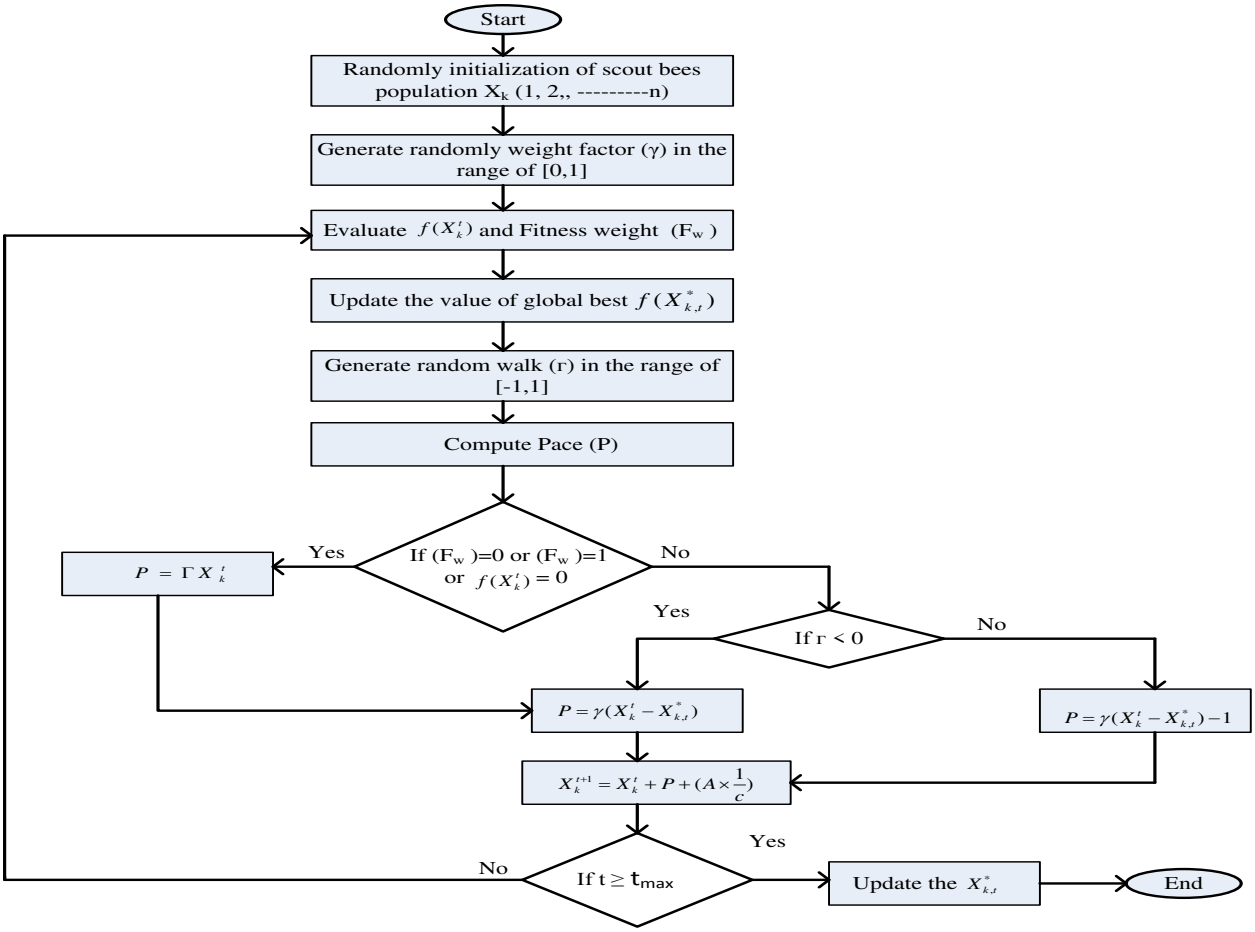

FIGURE 4. **Flow chart for the I-FDO algorithm.**

This article has been accepted for publication in a future issue of this journal, but has not been fully edited. Content may change prior to final publication. Citation information: DOI 10.1109/ACCESS.2020.3033983, IEEE Access

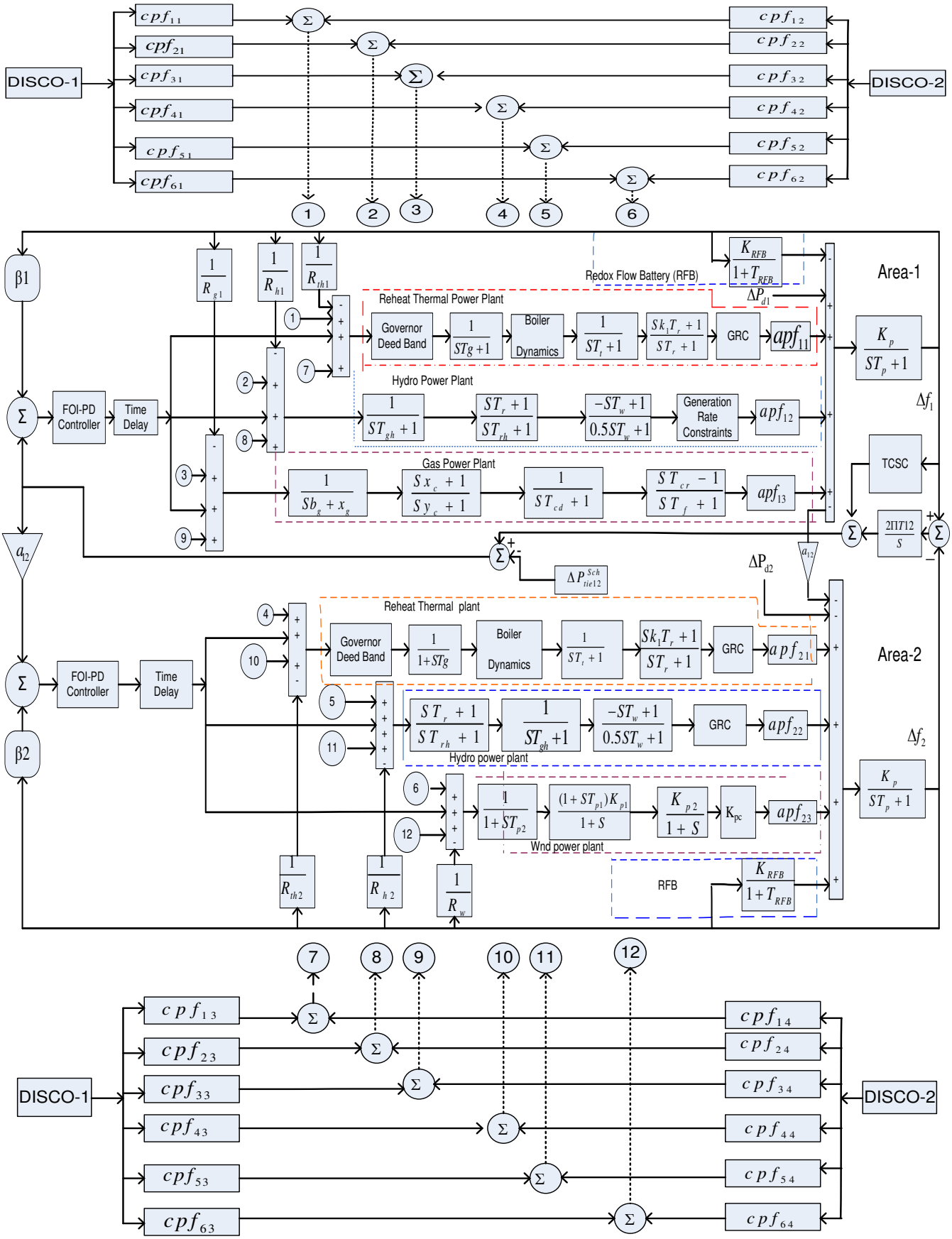

FIGURE 5. **Two areas multi-generation deregulated power system with non-linearities including TD, GRC, BD and GDB.**

This article has been accepted for publication in a future issue of this journal, but has not been fully edited. Content may change prior to final publication. Citation information: DOI 10.1109/ACCESS.2020.3033983, IEEE Access

TABLE 2. Parameters setting for controller under Poolco Based Transaction (PBT) considering different cases.

Controller Gains	Case-1				Case -2				Case-3			
	FOI-PD (I-FDO)	FOI-PD (FDO)	FOI-PD (TLBO)	FOI-PD (FA)	I-FDO (FOI-PD)	I-FDO (FOPID)	I-FDO (I-PD)	I-FDO (PID)	With RFB& TCSC	TCSC	RFB	Without RFB & TCSC
K_{p1}	1.176	1.010	1.091	1.130	1.290	1.405	1.032	0.998	1.678	1.340	1.458	1.009
K_{i1}	1.232	0.305	1.012	0.200	0.232	1.012	1.024	1.010	1.989	1.543	1.120	1.101
K_{d1}	1.190	0.011	-1.023	1.030	0.010	1.890	0.110	1.900	0.110	-0.220	1.456	1.988
λ_1	0.230	0.991	0.789	0.765	0.090	0.786	-	-	0.671	0.223	0.101	0.989
μ_1	0.002	0.910	0.675	0.003	0.002	0.344	-	-	0.678	0.972	0.234	0.760
K_{P2}	1.064	1.098	1.011	0.303	1.009	0.120	0.300	2.810	1.600	0.011	1.030	0.010
K_{i2}	1.040	1.023	1.304	1.109	-1.199	0.160	0.340	1.020	2.000	0.991	0.165	0.090
K_{d2}	1.200	1.100	1.008	1.001	1.560	0.305	1.090	1.200	1.078	-0.910	0.003	0.002
λ_2	0.090	0.786	0.165	0.090	0.099	0.001	-	-	0.899	0.165	0.671	0.213
μ_2	0.002	0.344	0.003	0.002	0.564	0.988	-	-	0.006	0.013	0.678	0.992
K_{p3}	0.948	2.000	1.903	0.789	1.230	1.200	1.234	1.876	1.124	0.898	1.234	1.678
K_{i3}	1.786	0.148	1.234	1.020	-1.11	1.456	1.987	1.002	1.001		1.298	1.200
K_{d3}	1.056	-1.001	1.678	0.789	1.098	1.011	0.303	1.009	1.064	1.098	1.011	1.004
λ_3	0.015	0.890	0.006	0.765	0.671	0.213	-	-	1.090	0.165	0.090	0.786
μ_3	0.013	0.102	0.124	0.013	0.678	0.992	-	-	1.898	0.003	0.002	0.344

TABLE 3. Parameters setting for controller with Bilateral Based Transaction (BBT) and Contract Violation Based Transaction (CVBT).

Controller Gains	Bilateral Based Transaction				Contract Violation Based Transaction			
	FOI-PD (I-FDO)	FOI-PD (FDO)	FOI-PD (TLBO)	FOI-PD (FA)	FOI-PD (I-FDO)	FOI-PD (FDO)	FOI-PD (TLBO)	FOI-PD (FA)
K_{p1}	1.678	1.989	1.543	1.120	1.101	1.064	1.032	0.998
K_{i1}	1.989	1.078	0.910	0.003	0.002	1.040	1.024	1.010
K_{d1}	0.110	-1.760	1.023	1.030	0.010	1.200	-0.110	1.900
λ_1	0.671	0.010	0.789	0.765	-0.090	0.190	0.189	0.100
μ_1	0.678	0.090	0.675	0.003	0.002	0.102	0.786	0.165
K_{P2}	1.290	0.450	0.032	0.303	1.009	0.420	0.300	2.810
K_{i2}	0.203	0.112	0.024	1.109	1.199	0.360	0.340	1.020
K_{d2}	-1.101	0.189	0.100	1.001	-1.560	0.005	1.090	1.200
λ_2	0.009	0.786	0.165	0.090	0.059	0.101	0.671	0.010
μ_2	0.767	0.344	0.003	0.002	0.564	0.188	0.678	0.090
K_{p3}	0.948	2.000	1.903	0.789	1.230	1.100	1.234	1.876
K_{i3}	1.786	0.148	1.234	1.020	1.111	-1.056	1.987	1.002
K_{d3}	1.064	-1.098	1.011	1.054	0.064	1.001	0.303	1.009
λ_3	0.899	0.165	0.671	0.165	0.601	0.003	0.110	0.330
μ_3	0.006	0.013	0.678	0.01s3	0.608	0.902	0.671	0.504

V. IMPLEMENTATION AND RESULTS

In this section, the model as shown in Figure 5 is developed in Matlab/Simulink using the values from Appendix (Table-1) and I-FDO algorithm is written in m. file. ITSE criteria are used as an objective function to tune the gains of the proposed controller. For the optimization of controller gains, the values of I-FDO parameters were taken from Appendix (Table 2). The optimization process has been performed 20 times for each algorithm, and the best optimal values among the 20 iterations are chosen as the controller's final gains. The optimal values for two areas six-generation unit in the deregulated environment under the Poolco Based Transaction (PBT) considering different cases are provided in Table 2. While the optimum values under Contract Violation Based Transaction (CVBT) and Bilateral Based Transaction (BBT) is presented in Table 3. The results attained from the proposed approach are associated with other algorithms such as FDO, FA and TLBO based FOI-PD algorithm. ITSE based convergence diagram of different algorithm is depicted in Figure 7. In order to evaluate the controller's efforts, the control signal

This article has been accepted for publication in a future issue of this journal, but has not been fully edited. Content may change prior to final publication. Citation information: DOI 10.1109/ACCESS.2020.3033983, IEEE Access

of FOPID and FOI-PD controllers using ITSE criteria are shown in Figure 9 which indicate that FOI-PD controller has high control signal as compared to FOPID controller.

A. POOLCO BASED TRANSACTION (PBT)

In PBT, Discos have a power contract with Gencos in their same control area. It is presumed that the two discos demands of 0.05 p.u.MW ($\Delta P_{L1} = \Delta P_{L2}$ =0.05 p.u.MW) power in control area1 from the Gencos of the similar control area. In the control area, 2 Discos have not any contract with Gencos i.e ($\Delta P_{L3} = \Delta P_{L4}$ =0.00 p.u.MW). Hence, the total load disturbance in area 1 is (ΔP_{d1} =0.1 p.u.MW) and in area 2 is (ΔP_{d2} =0.0 p.u.MW). A specific case of PBT between Gencos and Discos is simulated by considering below DPM.

$$DPM = \begin{bmatrix} 0.5 & 0.5 & 0.0 & 0.0 \\ 0.3 & 0.3 & 0.0 & 0.0 \\ 0.2 & 0.2 & 0.0 & 0.0 \\ 0.0 & 0.0 & 0.0 & 0.0 \\ 0.0 & 0.0 & 0.0 & 0.0 \\ 0.0 & 0.0 & 0.0 & 0.0 \end{bmatrix} \quad (40)$$

Three cases have been considered under PBT. The first case is the validation of the proposed I-FDO technique, which is compared with other optimized techniques such as FDO, TLBO and FA. In the second case, the performances of the novel proposed controller have been compared with the performance of other conventional controllers like FOPID, I-PD and PID. In the third case, the performance of the system has been evaluated with and without RFB and TCSC with prosed methods.

1) CASE-1

In case-1 the superiority of the proposed I-FDO technique has been validated by comparing the result with other optimization techniques including FDO, TLBO and FA. The dynamic response profile of the system with proposed techniques for 1% step load in area 1 under PBT is presented in Figure 6(a-c). It can be observed from Fig 6 (a-c) that I-FDO based optimization method quickly suppressed oscillation for frequency variation in area 1 (Δf_1), area 2 (Δf_2) and variation in tie-line power (ΔP_{tie}). A comprehensive comparative results for various algorithms in terms of Settling time (T_s), Overshoot (O_s) and Undershoot (U_s) for Δf_1 , Δf_2 and ΔP_{tie} are given in Table 4. From Fig 6 (a-c) it can be observed that FOI-PD controller tuned with I-FDO algorithm has nearly same peak overshoot as compared with FOI-PD tuned with FDO techniques but improved settling time by 11.95% for change in area-1 and 16.63% for change in area-2. Similarly, FOI-PD controller tuned with I-FDO improved settling time by (47.56%, 10.88% and 0.20%) and effectively reduced overshoot by (97.10%, 56.20%, and 69.41%) for Δf_1 , Δf_2 and ΔP_{tie} respectively as compared to FOI-PD controller tuned with FA. From Table 4, it can be observed that I-FDO based tuned FOI-PD controller as compared to hDE-PS based MID controller provides a significant improvement of 76.85%, 26.42% and 21.43% for both areas and in tie-line power, while effectively reduced peak overshoot of 97.80%, 85.88%, and 37.00% and undershoot of 6.00%, 70.13% and 75.00% for Δf_1 , Δf_2 and ΔP_{tie} respectively. Similarly, I-FDO based FOI-PD controller also provides an improvement of 53.62%, 4.96%, and 6.37% in T_s for load frequency of Δf_1 , Δf_2 and ΔP_{tie} respectively as compared hTLBO-PS based TID controller. From Fig 7 it can be seen that I-FDO algorithm converge rapidly by using ITSE criteria and obtained the value of (ITSE= 0.000168) as compared to FDO (ITSE=0.000290), TLBO (ITSE=0.000410) and FA (ITSE= 0.000513).

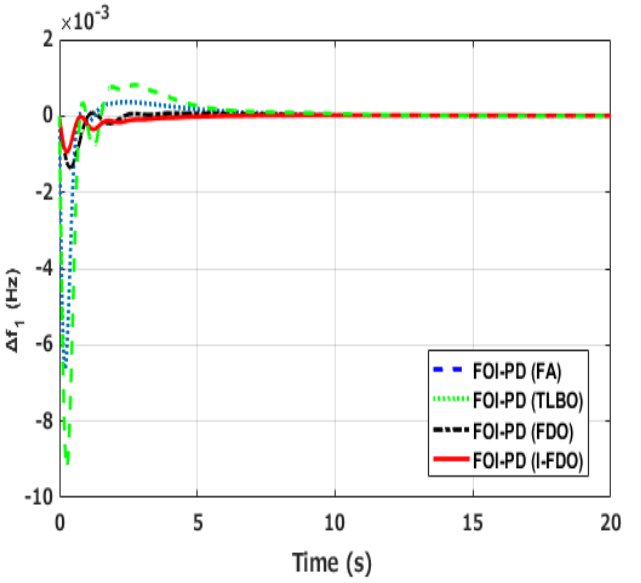

(a)

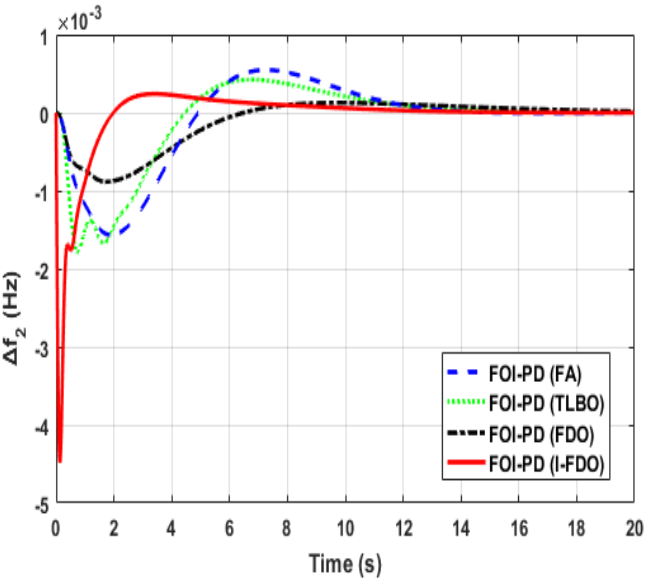

(b)

This article has been accepted for publication in a future issue of this journal, but has not been fully edited. Content may change prior to final publication. Citation information: DOI 10.1109/ACCESS.2020.3033983, IEEE Access

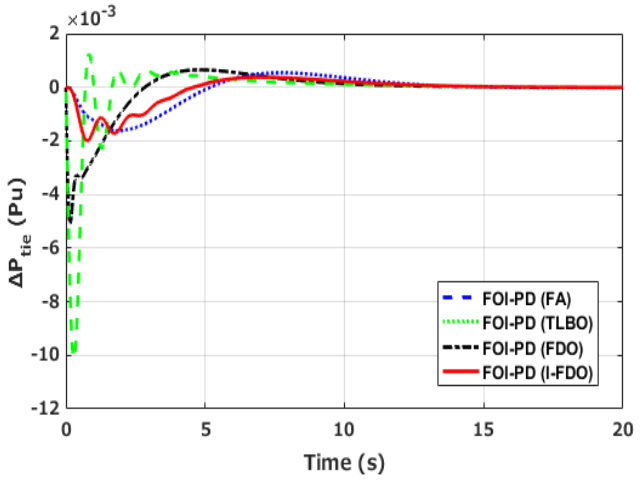

(c)

FIGURE 6. **Results under poolco based transaction considering case -1 for (a) Δf_1 (b) Δf_2 and (c) ΔP_{tie} .**

2) CASE-2

In this case, the performance of FOI-PD controller optimized with I-FDO algorithms have been compared with FO-PID, I-PD and PID controllers tuned with the same algorithm for two area multi-source IPS under poolco based transaction. The results obtained from the proposed techniques are shown in Figure 8(a-c) and Table 5. From Table 5 it can be seen that FOI-PD controller with I-FDO tuned method superiorly performs in respect of settling time by (2.80%, 16.56%, and 23.87%), overshoot by (69.36%, 62.55%, and 88.35%) for Δf_1 , Δf_2 and ΔP_{tie} respectively as compared to FOPID controller tuned with I-FDO techniques. From Fig 8(a-c) and Table 5 it can be observed that FOI-PD controller improved settling time by (42.84%, 10.65%, and 20.86%), effectively reduced peak overshoot by (49.56%, 89.24% and 95.40%) and reduced undershoot by (31.88%, 41.90% and 87.0%) for Δf_1 , Δf_2 and ΔP_{tie} respectively, when compared with PID controller optimized with similar algorithms.

Hence, it can be inferred that our proposed controller outperforms in respect of T_s, O_s and U_s as compared to PID and I-PD controllers optimized with a similar algorithm i.e. I-FDO.

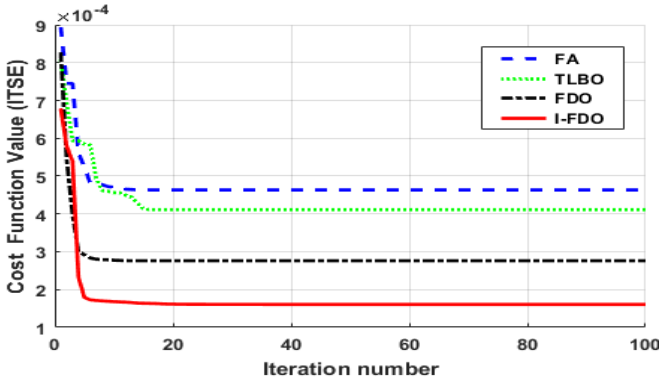

FIGURE 7. **Convergence diagram for different algorithms.**

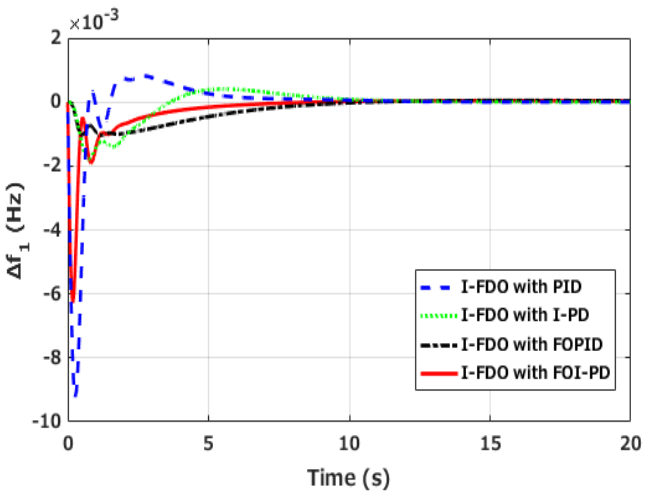

(a)

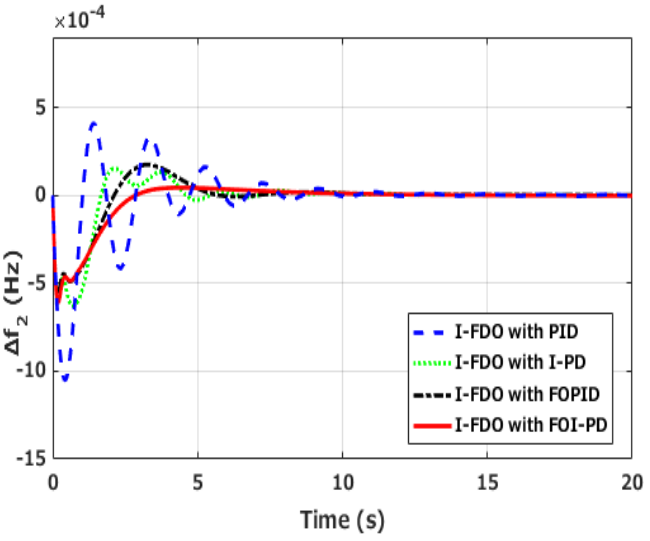

(b)

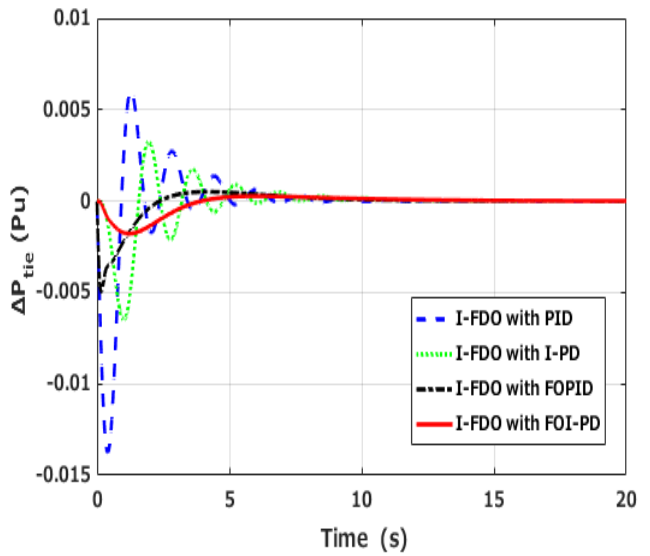

(c)

FIGURE 8. **Results under poolco based transaction considering case -2 for (a) Δf_1 (b) Δf_2 and (c) ΔP_{tie} .**

This article has been accepted for publication in a future issue of this journal, but has not been fully edited. Content may change prior to final publication. Citation information: DOI 10.1109/ACCESS.2020.3033983, IEEE Access

TABLE 4. Comparison performance of various algorithms under PBT for case-1 in terms of T_s, Os and Us.

Controller with Algorithms	T_s (Settling time)			O_s (Overshoot)			U_s (Undershoot)		
	Δf_1	Δf_2	ΔP_{tie}	Δf_1	Δf_2	ΔP_{tie}	Δf_1	Δf_2	ΔP_{tie}
FOI-PD (I-FDO)	**4.42**	**13.1**	9.97	**0.000017**	0.000240	**0.000378**	**-0.00094**	-0.00448	**-0.00199**
FOI-PD (FDO)	5.02	15.9	**9.81**	0.000082	0.000126	0.000651	-0.00135	**-0.00088**	-0.00507
FOI-PD (TLBO)	6.53	14.8	12.7	0.000363	0.000424	0.000542	-0.00664	-0.00178	-0.00162
FOI-PD (FA)	8.43	14.7	9.99	0.000813	0.000548	0.001236	-0.00922	-0.00156	-0.01012
TID (hTLBO-PS) [12]	9.53	13.75	10.36	0.007222	0.070400	0.003500	-0.18888	-0.24010	-0.06330
MID (hDE-PS) [20]	19.07	18.09	12.69	0.00080	0.001700	0.000600	-0.00100	-0.01500	-0.00800

TABLE 5. Comparison performance of the proposed algorithm with different controllers under PBT for case -2 in terms of T_s, Os and Us.

Controller with Algorithms	T_s (Settling time)			O_s (Overshoot)			U_s (Undershoot)		
	Δf_1	Δf_2	ΔP_{tie}	Δf_1	Δf_2	ΔP_{tie}	Δf_1	Δf_2	ΔP_{tie}
I-FDO with FOI-PD	**6.23**	**10.9**	**8.23**	**0.000041**	**0.000044**	**0.000272**	-0.00628	-0.00061	**-0.00178**
I-FDO with FOPID	7.93	11.1	8.46	0.000048	0.000174	0.000509	**-0.00104**	**-0.00056**	-0.00500
I-FDO with I-PD	8.61	11.0	9.02	0.000406	0.000153	0.003254	-0.00179	-0.00062	-0.00651
I-FDO with PID	10.9	12.2	10.4	0.000813	0.000409	0.006035	-0.00922	-0.00105	-0.01376

TABLE 6. Comparison performance under PBT for case-3 in terms of T_s, Os and Us.

Controller with Algorithms	T_s (Settling time)			O_s (Overshoot)			U_s (Undershoot)		
	Δf_1	Δf_2	ΔP_{tie}	Δf_1	Δf_2	ΔP_{tie}	Δf_1	Δf_2	ΔP_{tie}
I-FDO with RFB& TCSC	**8.10**	**6.23**	**10.8**	**0.000115**	**0.000039**	**0.00116**	**-0.00446**	-0.00527	**-0.00681**
I-FDO with TCSC	9.80	7.80	11.2	0.000508	0.000318	0.00223	-0.00912	**-0.00441**	-0.00685
I-FDO with RFB	9.90	8.20	11.8	0.000557	0.000319	0.00224	-0.00691	-0.00568	-0.00812
FDO without RFB&TCSC	11.8	12.4	12.1	0.001410	0.001641	0.00363	-0.01023	-0.00695	-0.00823

3) CASE-3

In case 3, the effect of introducing RFB and TCSC unit on AGC is investigated. RFB unit is incorporated in each area and TCSC is considered in tie-line of the system. The performance of the system is evaluated with I-FDO based FOI-PD controller considering the effect of RFB, TCSC, both RFB and TCSC and without RFB and TCSC. The results attained for Δf_1 , Δf_2 and ΔP_{tie} are shown in Figure 10 (a-c). From Fig 10 (a-c) it can be observed that performance of the proposed techniques including TCSC and RFB unit is superior as compared to without considering TCSC and RFB for Δf_1 , Δf_2 and ΔP_{tie} in terms of T_s, O_s and U_s. The dynamic response of the system incorporated with TCSC and RFB unit is improved in respect of settling time by (11.30%, 12.96%, and 23.56%), reduced overshoot by (55.67%, 47.78% and 34.89 %) and undershoot by (14.50%, 11.08% and 2.09%) for Δf_1 , Δf_2 and ΔP_{tie} respectively as compared to a system without considering the effect of RFB and TCSC unit. From Fig 10 (a-c) and Table 6 it is seen that the response of the system considering the individual effect of TCSC and RFB is improved in respect of T_s, O_s and U_s as compared to without including the effect of TCSC and RFB unit for Δf_1 , Δf_2 and ΔP_{tie} . Hence, it can be concluded from Table 6 that our proposed techniques perform outstanding incorporating with RFB and TCSC.

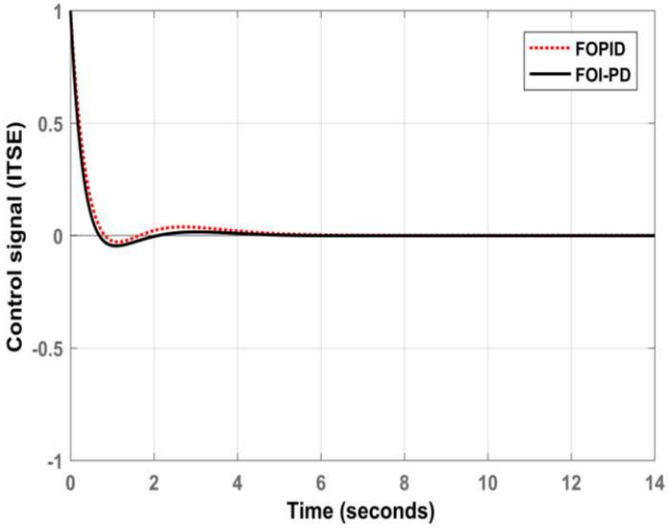

FIGURE 9. **Control signals for FOPID and FOI-PD controllers.**

This article has been accepted for publication in a future issue of this journal, but has not been fully edited. Content may change prior to final publication. Citation information: DOI 10.1109/ACCESS.2020.3033983, IEEE Access

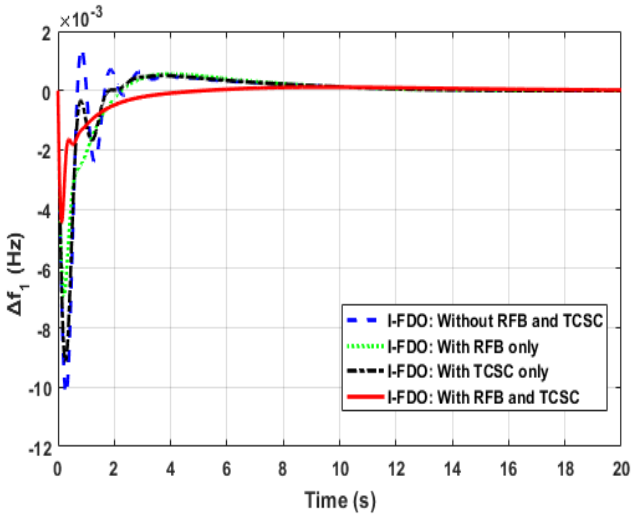

(a)

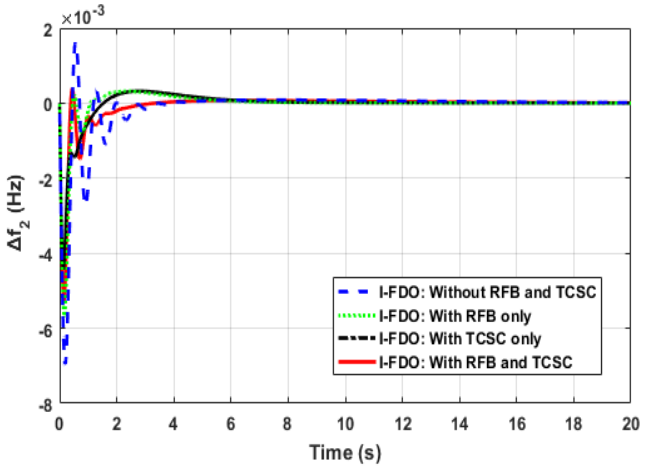

(b)

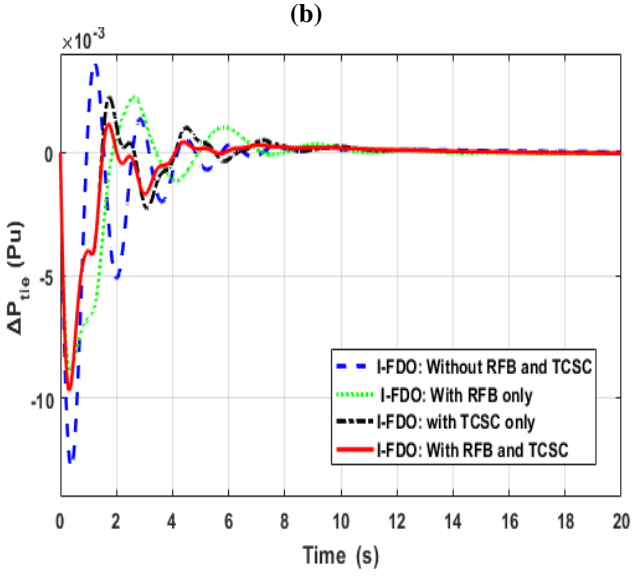

(c)

FIGURE 10. **Results under poolco based transaction considering case - 3 for (a) Δf_1 (b) Δf_2 and (c) ΔP_{tie} .**

B. BILATERAL BASED TRANSACTION (BBT)

In BBT, Discos have a power contract with Gencos in their same or different control area. It is presumed that each Discos demand of 0.05 p.u.MW ($\Delta P_{L1} = \Delta P_{L2} = \Delta P_{L3} = \Delta P_{L4}$ =0.05 p.u.MW) power in both areas and hence, the entire load disturbance in area 1 is (ΔP_{d1} =0.1 p.u.MW) and in area 2 is (ΔP_{d2} =0.1 p.u.MW). All Gencos participated in AGC task can be represented by below DPM.

$$DPM = \begin{bmatrix} 0.2 & 0.10 & 0.3 & 0.00 \\ 0.2 & 0.25 & 0.1 & 0.16 \\ 0.1 & 0.25 & 0.2 & 0.16 \\ 0.2 & 0.10 & 0.2 & 0.36 \\ 0.1 & 0.20 & 0.1 & 0.16 \\ 0.1 & 0.10 & 0.1 & 0.16 \end{bmatrix} \tag{41}$$

The response of the system under BBT is given in Figure 11 (a-c) and the overall comparison of mentioned techniques in terms of T_s, O_s and U_s for Δf_1 , Δf_2 and ΔP_{tie} respectively is shown in Table 7. When comparing the settling time (T_s) of Fig 11 (a-c), the proposed I-FDO tuned FOI-PD controller has quickly reached the T_s as 12.63%, 34.56% and 23.67% is compared to FOI-PD controller tuned with FA algorithm. When comparing the undershoot (U_s) of FA tuned FOI-PD controller, the proposed FOI-PD controller optimized with I-FDO techniques has efficiently reduced the U_S as 78.30%, 45.67% and & 49.30% as compared to FA tuned FOI-PD controller. When comparing the overshoot (O_s) of Fig 11 (a-c)), the proposed I-FDO optimized FOI-PD controller has efficiently reduced the overshoot as 56.03%, 78.06% and 48.69% is compared to FOI-PD controller tuned with FA algorithm. Hence, it can be inferred, that I-FDO based FOI-PD controller has better performance in terms of T_s, O_s and U_s for Δf_1 , Δf_2 and ΔP_{tie} respectively as compared to FOPID controller optimized with FDO/TLBO/FA.

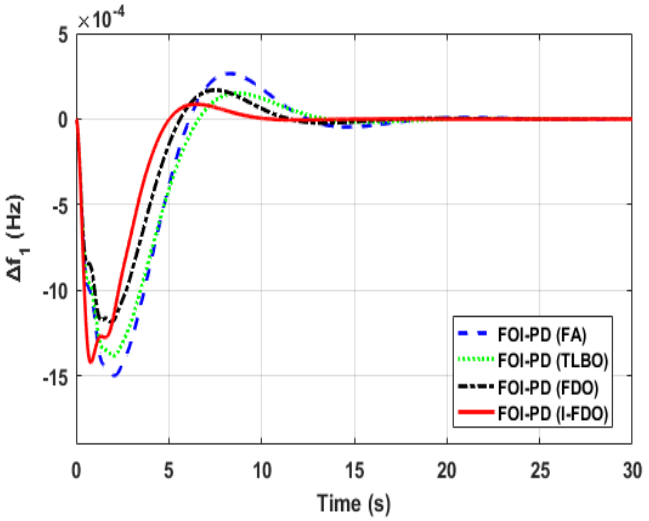

(a)

This article has been accepted for publication in a future issue of this journal, but has not been fully edited. Content may change prior to final publication. Citation information: DOI 10.1109/ACCESS.2020.3033983, IEEE Access

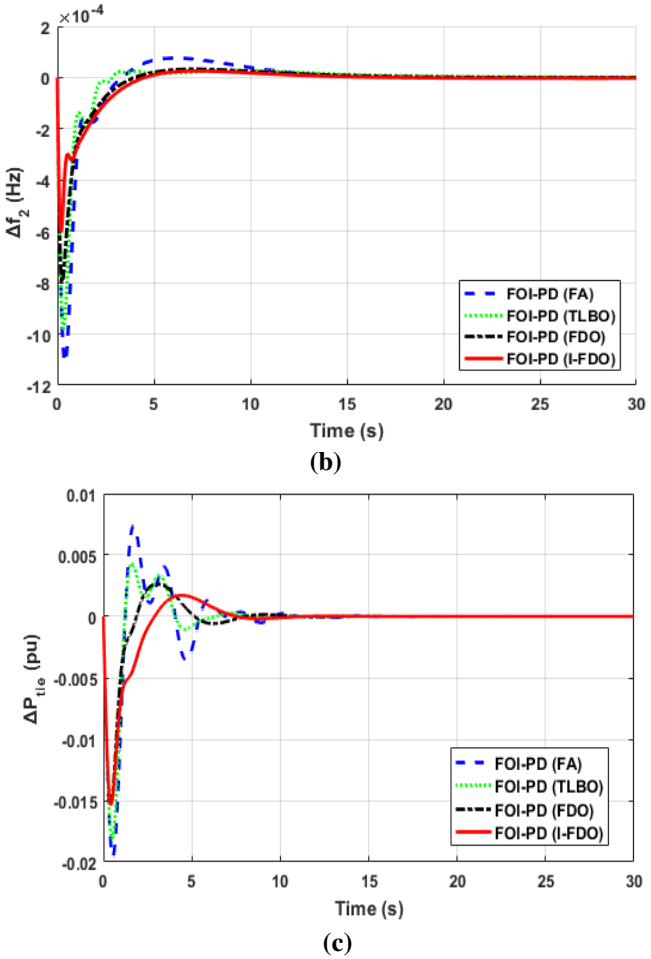

FIGURE 11. **Results under bilateral based transaction for (a)** Δf_1 **(b)** Δf_2 **and (c)** ΔP_{tie} **.**

C. CONTRACT VIOLATION BASED TRANSACTION (CVBT)

In contract violation, Discos need more power than a specified contract which is not contracted out to any Gencos. This uncontracted power must be provided by Gencos to Discos in the similar area. In this scenario, a poolco based transaction is again considered with modification of 10% excess uncontracted power i.e (ΔP_{uc1} =0.1pu.MW) demanded by Disco-1 from area-1 and (ΔP_{uc2} =0.0 pu.MW) from area 2. So, the total load demand (ΔP_{d1}) in Area -1= $\Delta P_{L1} + \Delta P_{L2} + \Delta P_{uc1}$ =0.1+0.1+0.1= 0.3 p.u.MW. Whereas $\Delta P_{d2} = \Delta P_{L3} + \Delta P_{L4} + \Delta P_{uc2}$ =0.1+0.1+0=0.2 p.u.MW. Under contract violation, the dynamic profile of the system is shown in Figure 12 (a)-(c). From Table 8 it can be seen that FOI-PD controller with I-FDO tuned method superiorly performs in respect of T_s by (10.34%, 09.54%, and 31.76%), O_s by (78.77%, 57.76%, and 89.36%) and U_s by (14.56%, 3.09%, and 19.56%) for Δf_1 , Δf_2 and ΔP_{tie} respectively as compared to FOI-PD controller tuned with FDO optimization techniques. Similarly, when comparing the overshoot (O_s) of Fig 12 (a-c)), the proposed I-FDO optimized FOI-PD controller has efficiently reduced the overshoot as 76.22%, 28.16% and 83.32% is compared to FOI-PD controller tuned with FA algorithm. The settling time of I-FDO optimized FOI-PD controller is improved by (39.12%, 12.08%, and 41.63%) for Δf_1 , Δf_2 and ΔP_{tie} respectively as compared to FOI-PD controller tuned with FA algorithm.

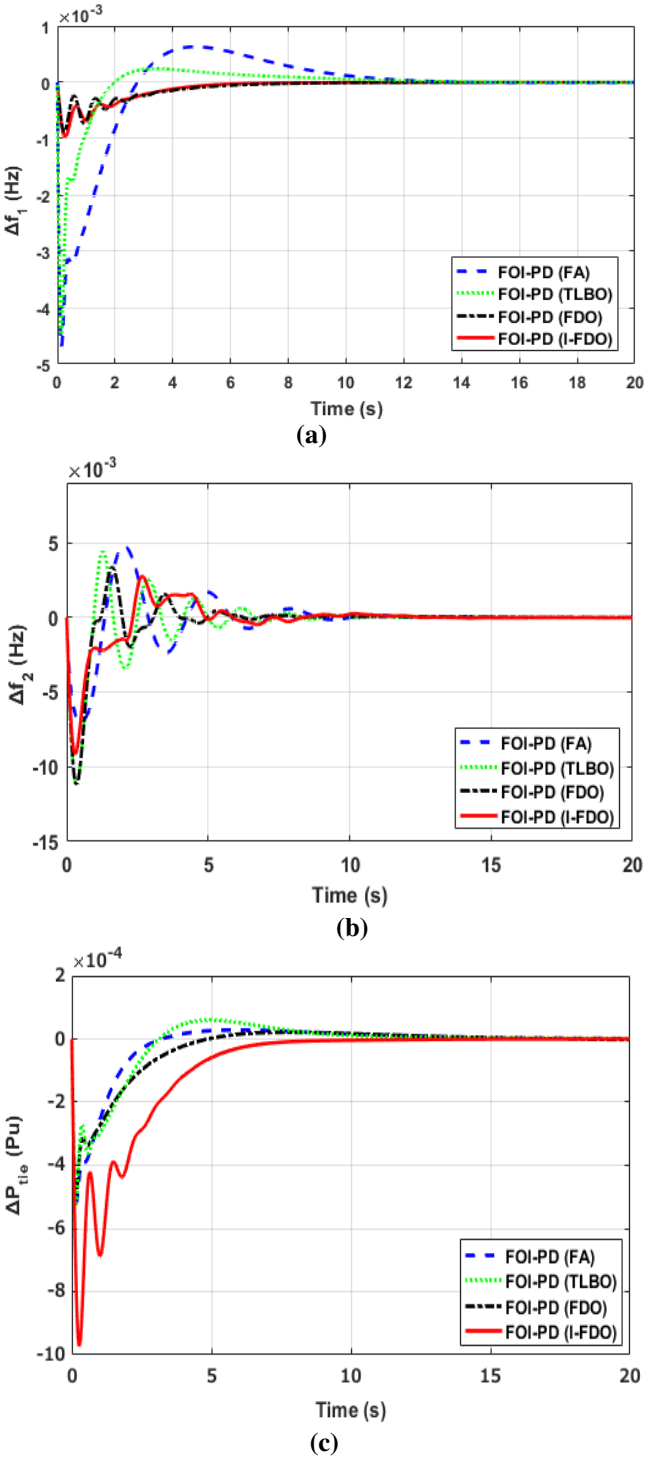

FIGURE 12. **Results under contract violation based transaction for (a)** Δf_1 **(b)** Δf_2 **and (c)** ΔP_{tie} **.**

This article has been accepted for publication in a future issue of this journal, but has not been fully edited. Content may change prior to final publication. Citation information: DOI 10.1109/ACCESS.2020.3033983, IEEE Access

D. SENSITIVITY \ ROBUSTNESS ANALYSIS

Sensitivity analysis is performed to examine the uncertainty of power system in dynamic behaviour under a nominal condition concerning a certain change in a few of the essential parameters of the system. The purpose of this analysis is to study the robust performance of the controller by varying system parameters. This paper has carried out a sensitivity analysis of the some of the system parameters with nominal value by varying the turbine time constant (T_g), synchronizing coefficient (T_{12}), droop constant (R) and governor time constant (T_t) in the range of ± (25%). The results obtained by varying system parameters in the range of ± (25) % are shown in Figure 13 (a) - (g). The comparison of various parameters in terms of settling time, undershoot and overshoot with a change of ± (25) % from their nominal values are provided in Table 9. From Fig 13 (a-g), it can be observed that the response of the system plotted for various parameters are almost similar to the nominal values which show that the proposed I-FDO based FOI-PD controller provides a robust performance within a range of ± (25) % of the system parameters. Furthermore, the optimized values of the proposed controller don't need to be re-tuned for wide-ranging parameters attained at nominal load with nominal parameters.

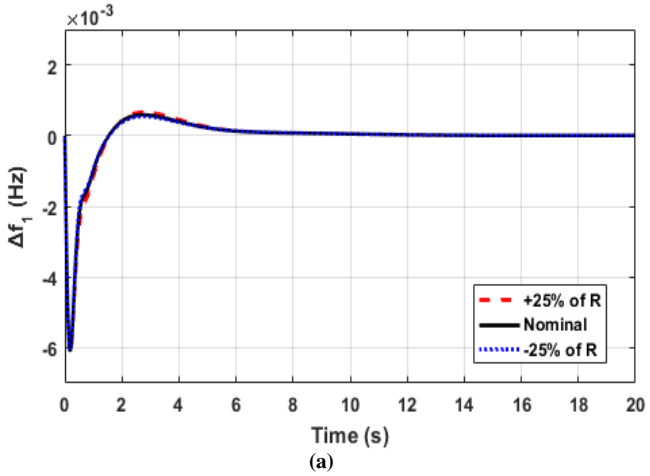

(a)

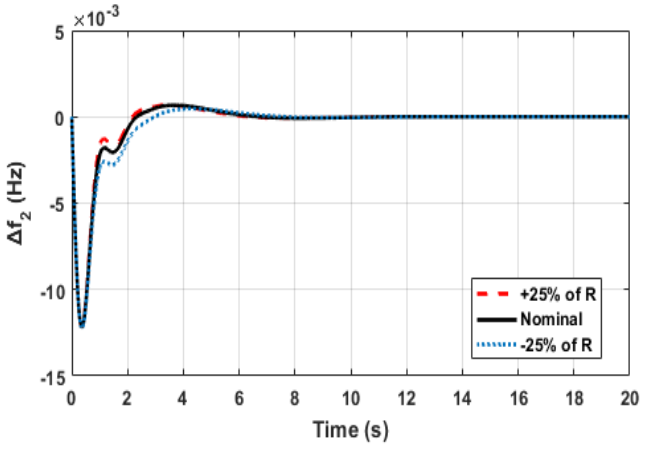

(b)

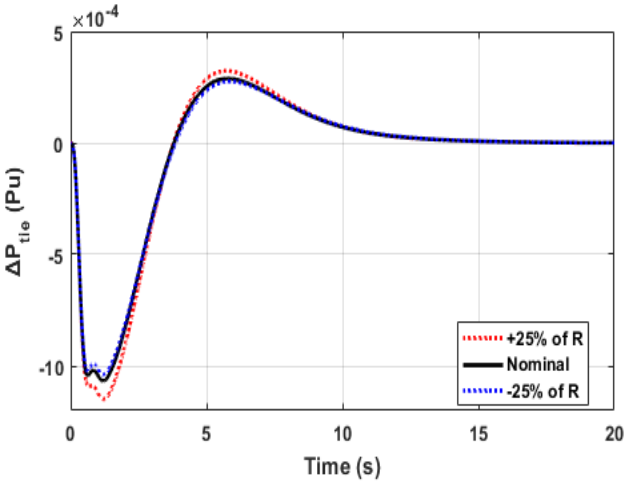

(c)

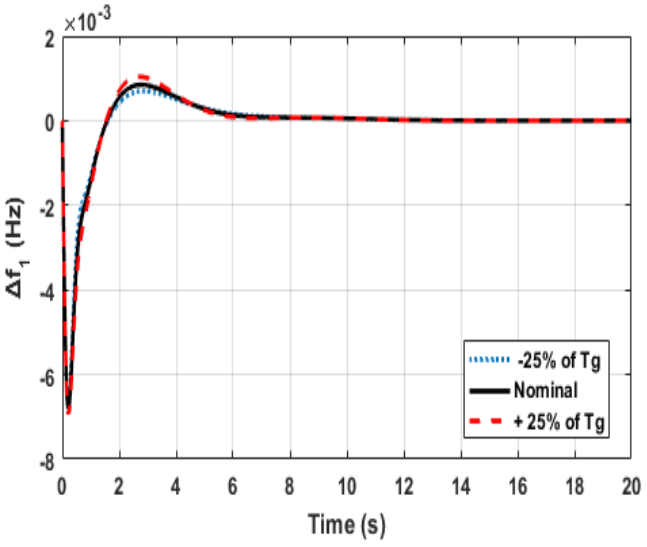

(d)

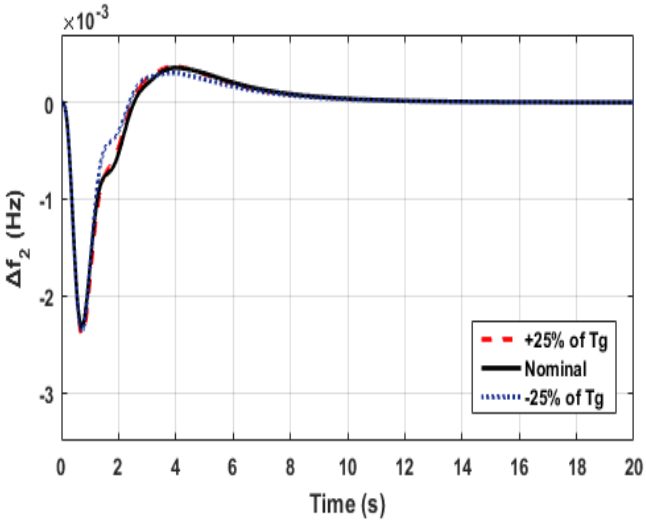

(e)

This article has been accepted for publication in a future issue of this journal, but has not been fully edited. Content may change prior to final publication. Citation information: DOI 10.1109/ACCESS.2020.3033983, IEEE Access

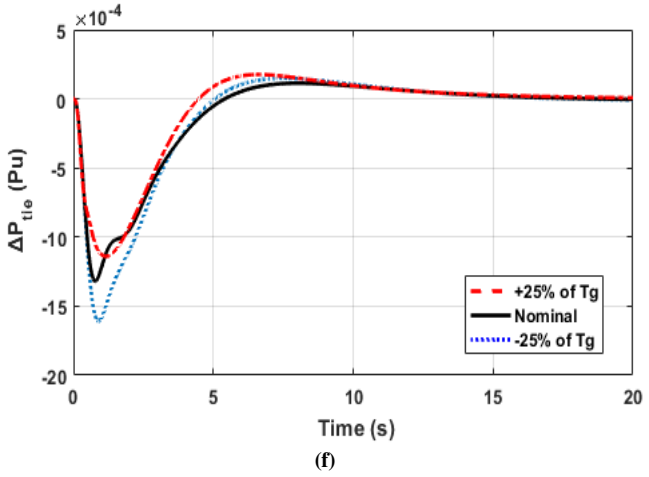

(f)

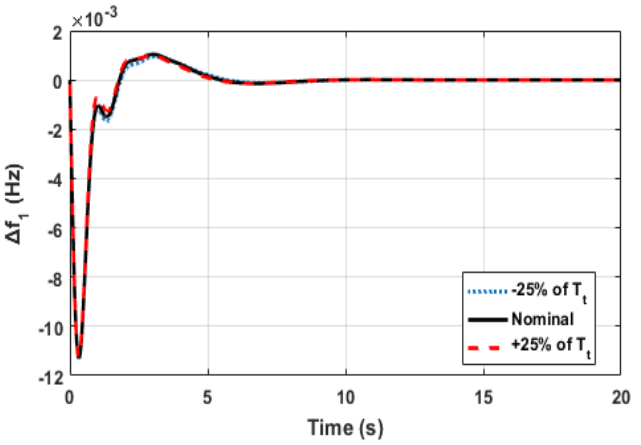

(g)

FIGURE 13. **The response of the system with a variation of (a) R with Δf_1 b) R with Δf_2 (c) R with ΔP_{tie} (d) T_g with Δf_1 e) T_g with Δf_2 (f) T_g with ΔP_{tie} (g) T_t with Δf_1 ΔP_{tie} .**

TABLE 7. Comparison performance under BBT in terms of T_s, O_s and U_s.

Controller with Algorithms	T_s (Settling time)			O_s (Overshoot)			U_s (Undershoot)		
	Δf_1	Δf_2	ΔP_{tie}	Δf_1	Δf_2	ΔP_{tie}	Δf_1	Δf_2	ΔP_{tie}
FOI-PD (I-FDO)	**17.6**	**18.3**	**11.7**	**0.000085**	**0.0000257**	0.00171	-0.00410	**-0.00060**	-0.0151
FOI-PD (FDO)	18.2	19.4	12.8	0.000168	0.0000326	0.00262	-0.00117	-0.00080	-0.0151
FOI-PD (TLBO)	21.1	19.9	13.2	0.000151	0.0000276	0.00429	-0.00137	-0.00098	-0.0180
FOI-PD (FA)	23.2	12.1	14.1	0.000225	0.0000765	0.00741	-0.00149	-0.00111	-0.0195
TID (hTBO-PS)[12]	27.99	26.17	12.30	0.0599	0.05910	0.00116	-0.39500	-0.42160	**-0.0123**
MID (hDE-PS) [20]	20.15	18.58	14.22	0.0010	0.001600	**0.00090**	**-0.00100**	-0.00150	-0.0800

TABLE 8. Comparison performance under contract violation in terms of T_s, O_s and U_s.

Controller with Algorithms	T_s (Settling time)			O_s (Overshoot)			U_s (Undershoot)		
	Δf_1	Δf_2	ΔP_{tie}	Δf_1	Δf_2	ΔP_{tie}	Δf_1	Δf_2	ΔP_{tie}
FOI-PD (I-FDO)	**11.02**	**13.8**	**12.80**	**0.000000**	0.00273	**0.000000**	**-0.00097**	**-0.00681**	**-0.00097**
FOI-PD (FDO)	11.09	13.9	13.30	0.000000	0.00335	0.000021	-0.00088	-0.00685	-0.00049
FOI-PD (TLBO)	16.4	17.3	14.47	0.000631	0.00442	0.000028	-0.00468	-0.00812	-0.00052
FOI-PD (FA)	16.9	17.7	15.36	0.000241	0.00473	0.000060	-0.00448	-0.00823	-0.00053
TID (hTBO-PS)[12]	24.50	24.62	18.78	0.023100	0.03520	0.039000	-0.54960	-0.68980	-0.07590
MID (hDE-PS) [20]	24.31	22.72	19.05	0.001600	**0.00210**	0.001000	-0.00234	-0.00956	-0.01890

TABLE 9. Results of Sensitivity analysis for proposed I-FDO based FOI-PD controller considering PBT.

Parameter	% Change	T_s (Settling time)			O_s (overshoot)			U_s (Undershoot)		
		Δf_1	Δf_2	ΔP_{tie}	Δf_1	Δf_2	ΔP_{tie}	Δf_1	Δf_2	ΔP_{tie}
R	**+25**	6.78	6.38	12.72	0.00064	0.00068	0.000323	-0.00610	-0.00240	-0.00315
	-25	7.90	8.01	12.73	0.00054	0.00047	0.000276	-0.00600	-0.00236	-0.00313
Tg	**+25**	6.74	6.38	13.01	0.00094	0.00037	0.000296	-0.00693	-0.00713	-0.00489
	-25	7.91	8.03	13.03	0.00098	0.00030	0.000289	-0.00678	-0.00913	-0.00482
Tt	**+25**	6.14	6.10	12.80	0.00083	0.00014	0.000310	-0.00731	-0.00780	-0.00361
	-25	8.10	7.80	12.79	0.00075	0.00017	0.000311	-0.00725	-0.00740	-0.00361
T_{12}	**+25**	6.17	6.09	13.10	0.00063	0.00032	0.000315	-0.00623	-0.00830	-0.00251
	-25	8.10	7.82	13.08	0.00061	0.00031	0.000316	-0.00618	-0.00840	-0.00257

This article has been accepted for publication in a future issue of this journal, but has not been fully edited. Content may change prior to final publication. Citation information: DOI 10.1109/ACCESS.2020.3033983, IEEE Access

VI. CONCLUSION

In this paper, FOI-PD controller is designed and developed for AGC of two areas, six-generation units under the deregulated environment with the inclusion of various non-linearities including GDB, BD, TD and GRC. Improved–Fitness Dependent Optimizer (I-FDO) meta-heuristic algorithm is used to optimize the parameters of the proposed controller. In addition, the dynamic response of the system is improved by Incorporating RFB in each area and TCSC in series with the tie-lines. From simulation results, it can be observed that I-FDO based tuned FOI-PD controller as compared to hDE-PS based MID controller provides a significant improvement of 76.85%, 26.42% and 21.43% for both areas and in tie-line power, while effectively reduced peak overshoot of 97.80%, 85.88%, and 37.00% and undershoot of 6.00%, 70.13%, 75.00% for Δf_1, Δf_2 and ΔP_{tie} respectively. Similarly, I-FDO based FOI-PD controller also provides an improvement of 53.62%, 4.96%, and 6.37% in T_s for load frequency of Δf_1, Δf_2 and ΔP_{tie} respectively as compared hTLBO-PS based TID controller. Finally, the robustness of FOI-PD controller is evaluated by varying the system parameters from nominal values and the results show that the gains of the FOI-PD controller have not been reset when the system parameters or load conditions changed. The efficacy of I- FDO based FOI-PD controller exhibits the ability of the controller to efficiently handle AGC problems under a deregulated environment promptly with sustained oscillations.

APPENDIX

TABLE 1. Parameter setting for two-area interconnected power system [39].

Parameters	Values	Parameters	Values	Parameters	Values
$\beta_1$and β_2	0.4312 p.u. MW/Hz	R_{th1}, R_{th2}, R_{hy1}, R_{hy2}, R_{g1}, R_{w1}	2.4 Hz/p.u	T_{gh}	0.08 s
T_t	0.3 s	K_1	0.3	T_r	10 s
K_P	68.956	T_p	11.49 s	T_{12}	0.0433
a_{12}	-1	T_w, y_c	1 s	T_{rs}	5 s
T_{rh}	28.75 s	T_{gh}, T_{cd}, T_{DC}	0.2 s	x_c	0.6 s
K_g	0.130438	K_{DC}, x_g	1	b_g	0.05 s
K_t	0.543478	T_{cr}	0.01 s	T_f	0.23 s
K_{p1}	1.25	K_{p2}	1.4	T_{p1}	0.6
T_{p2}	0.041	K_{RFB}	0.67	T_{RFB}	0 s
K_h	0.85	K_c	0.8243	K_b	0.950
K_{pc}	0.8				

TABLE 2. Values of I-FDO parameters.

Parameters	Values	Parameters	Values	Parameters	Values	Parameters	Values
Number of Population (Np)	30	Number of generations (Ng)	100	Lower bound	-2	Upper bound	2
Number of dimension	5	random number (Γ)	[-1 1]	Weight factor (ϒ)	[0,1]		

REFERENCES

[1] K. S. Rajesh, S. S. Dash, and R. Rajagopal, "Hybrid improved firefly - pattern search optimized fuzzy aided PID controller for automatic generation control of power systems with multi-type generations," *Swarm Evol Comput.,* vol. 44, pp. 200-211, Feb. 2019.

[2] Y. Arya, "Improvement in automatic generation control of two-area electric power systems via a new fuzzy aided optimal PIDN-FOI controller," ISA Trans., vol. 80, pp. 475-490, Sep. 2018.

[3] Z. Bingul and O. Karahan, "A novel performance criterion approach to optimum design of PID controller using cuckoo search algorithm for AVR system," Journal of the Franklin Institute, Vol. 355, Issue 13,2018, PP 534-559, https://doi.org/10.1016/j.jfranklin.2018.05.056.

[4] N. Mahendra, C.K. Shiva b, V. Mukherjee, TCSC based automatic generation control of deregulated power system using quasi-oppositional harmony search algorithm," *Engineering Science and Technology an International Journal.,* vol. 20, pp. 1380–1395, 2017.

[5] A. Pappachen, and A. P. Fathima, NERC's control performance standards-based load frequency controller for a multi-area deregulated power system with ANFIS approach," *Ain Shams Engineering Journal*., 2017.

[6] U. Raj, and R. Shankar, "Deregulated Automatic Generation Control using Novel oppositional based Interactive Search Algorithm Cascade Controller Including Distributed Generation and Electric Vehicle. Iranian Journal of Science and Technology," *Trans of Electrical Engineering.,* vol. 44, pp. 1233–1251, 2020.

[7] A. Daraz, S. A. Malik and A. ul Haq, "Review of Automatic Generation Control For Multi-Source Interconnected Power System Under Deregulated Environment," International Conference on Power Generation Systems and Renewable Energy Technologies (PGSRET), Islamabad, Pakistan, pp. 1-5, 2018.

[8] V. Donde, M. A. Pai, and I. A. Hiskens, "Simulation and optimization in an AGC system after deregulation,' *IEEE Trans Power Sys.,* vol. 16, pp.481–491, 2011.

[9] K. P .S Parmar, S. Majhi, and D. P. Kothari, "LFC of an interconnected power system with multi-source power generation in deregulated power environment," *Int J Elect Power Energy Syst*., vol. 57, pp. 277–286, 2014.

[10] A. Demiroren, and H. L. Zeynelgil, "GA application to optimization of AGC in three-area power system after deregulation," *Int J ElectPower Energy Syst., vol.* 29, pp. 230–240, 2007.

[11] S. Debbarma, L. C. Saikia, and N. Sinha, "AGC of a multi-area thermal system under deregulated environment using a non-integer controlle," *.Electric Power Syst Res*., vol. 95, pp. 175–183, 2013.

[12] D. Khamari, R. K. Sahu, T. S. Gorripotu, and S. Panda, "Automatic generation control of power system in deregulated environment using hybrid TLBO and pattern search technique," *Ain Shams Engineering Journal.*, Oct 2019.

[13] R. Shankar, A. Kumar, U. Raj, and K. Chatterjee, "Fruit fly algorithm-based automatic generation control of multi-area interconnected power system with FACTS and AC/DC links in deregulated power environment," *Int Trans Electrical Energy Syst*., vol. 29, pp. 1–25,2019.

[14] C. K. Shiva, and V. Mukherjee, "A novel quasi-oppositional harmony search algorithm for AGC optimization of three-area multi-unit power system after deregulation," *Eng Sci Technol Int*., vol. 19 pp. 395–420,2015.

[15] R.J. Abraham, D. Das, A. Patra, Effect of TCPS on oscillations in tie-power and area frequencies in an interconnected hydrothermal power system, *IET Gener. Trans. Distrib.,* vol. pp. 632–639, 2007.

[16] A. Prakash, S. Murali, R. Shankar, R. Bhushan, S. Padhan, R. K. Sahu, and S. Panda, "Automatic generation control with thyristor controlled series compensator including superconducting magnetic energy storage units," *Ain Shams Eng J.,* vol. 5, pp. 759–774,2014.

[17] M. Ponnusamy, B. Banakara, S. S. Dash, and M. Veerasamy, "Design of integral controller for load frequency control of static synchronous series compensator and capacitive energy source based multi area system consisting of diverse sources of generation employing imperialistic competition algorithm,"*Int Journal of Electrical Power & Energy Systems.*, vol. 73, pp. 863–871, 2015.

[18] P.C. Pradhan, R.K. Sahu, and S. Panda, "Firefly algorithm optimized fuzzy PID controller for AGC of multi-area multi-source power systems with UPFC and SMES," *Eng. Sci. Tech.,* vol. 19, pp. 338–354, 2016.

[19] Y. Arya, and N. Kumar, "Optimal AGC with redox flow batteries in multi-area restructured power systems," *Eng. Sci. Technol*., 2016.

[20] R.K. Sahu, T.S. Gorripotu, S. Panda, "A hybrid DE-PS algorithm for load frequency control under deregulated power system with UPFC and RFB," *Ain Shams Eng. J.,* no. 3, vol. 6, pp. 893–911, 2015.

[21] I. A. Chidambaram, and B. Paramasivam, "Optimized load-frequency simulation in restructured power system with redox flow batteries and interline power flow controller*," Int. J. Electr. Power Energy Syst*., vol. pp. 9–24, 2013.

[22] T. S. Gorripotu, R.K. Sahu, S. Panda, "AGC of a multi-area power system under deregulated environment using redox flow batteries and interline power flow controller," *Eng. Sci. Technol.,* no. 4, vol. 18 pp. 555–578,2015.

[23] K. Zare, M. T. Hagh, and J. Morsali, "Effective oscillation damping of an interconnected multi-source power system with automatic generation control and TCSC," I*nt. J. Electr. Power Energy Syst., vol. 65*, pp. 220–230, 2015.

[24] M. Deepak, and R. J. Abraham, Load following in a deregulated power system with thyristor controlled series compensator," *Int. J. Electr. Power Energy Syst*., vol. 65 pp. 136–145, 2015.

[25] E. Sahin, "Design of an Optimized Fractional High Order Differential Feedback Controller for Load Frequency Control of a Multi-Area Multi-Source Power System With Nonlinearity," in IEEE Access, vol. 8, pp. 12327-12342, 2020, doi: 10.1109/ACCESS.2020.2966261.

[26] H. M. Hasanien. "Whale optimisation algorithm for automatic generation control of interconnected modern power systems including renewable energy sources," *IET Gener., Transmiss. Distrib.*,vol. 12, no. 3, pp. 607-614, Feb. 2018.

[27] W. Tasnin, and L. C. Saikia, "Maiden application of an sine-cosine algorithm optimized FO cascade controller in automatic generation control of multi-area thermal system incorporating dish-stirling solar and geothermal power plants," *IET Renewable Power Generation.,* vol. 12, no. 5, pp. 585–597,2018

[28] Y. Arya, "A novel CFFOPI-FOPID controller for AGC performance enhancement of single and multi-area electric power systems," *ISA Transactions.,* vol. 100, pp. 126–135, 2020.

[29] J. Morsali, K. Zare, and M. T. Hagh, "A novel dynamic model and control approach for SSSC to contribute effectively in AGC of a deregulated power system," *Electrical Power and Energy Systems.,* vol. 95, pp. 239–253, 2018

[30] A. Daraz, S. A. Malik, H. Mokhlis, I. U. Haq, G. F. Laghari and N. N. Mansor, "Fitness Dependent Optimizer-Based Automatic Generation Control of Multi-Source Interconnected Power System With Non-Linearities," in IEEE Access, vol. 8, pp. 100989-101003, 2020, doi: 10.1109/ACCESS.2020.2998127.

[31] G. Chen, Z. Li, Z. Zhang and S. Li, "An Improved ACO Algorithm Optimized Fuzzy PID Controller for Load Frequency Control in Multi Area Interconnected Power Systems," in IEEE Access, vol. 8, pp. 6429-6447, 2020, doi: 10.1109/ACCESS.2019.2960380.

[32] H. M. Hasanien and A. A. El-Fergany, ``Salp swarm algorithm-based optimal load frequency control of hybrid renewable power systems with communication delay and excitation cross-coupling effect," Electr. Power Syst. Res., vol. 176, Nov. 2019, Art. No. 105938.

[33] V. Veerasamy et al., "A Hankel Matrix Based Reduced Order Model for Stability Analysis of Hybrid Power System Using PSO-GSA Optimized Cascade PI-PD Controller for Automatic Load Frequency Control," in IEEE Access, vol. 8, pp. 71422-71446, 2020, doi: 10.1109/ACCESS.2020.2987387.

[34] P. C. Sahu1, R. C. Prusty, and S. Panda, "Improved-GWO designed FO based type-II fuzzy controller for frequency awareness of an AC micro grid under plug in electric vehicle," *Journal of Ambient Int and Humanized Computing.*, Mar 2020,doi: 10.1007/s12652-020-02260-z.

[35] A. Prakash, S. Murali, R. Shankar, R. Bhushan, "HVDC tie-link modeling for restructured AGC using a novel fractional order cascade controller," *Electric Power Systems Research.,vol.* 170, pp. 244–258, 2019. https://doi.org/10.1016/j.epsr.2019.01.021.

[36] Y. Arya, "Impact of ultracapacitor on automatic generation control of electric energy systems using an optimal FFOID controller," Int J Energy Res., vol. 43, pp. 8765–8778, 2019.

[37] Y. Arya, "AGC of restructured multi-area multi-source hydrothermal power systems incorporating energy storage units via optimal fractional-order fuzzy PID controller," Neural Comput. Appl., no. 3, vol. 31, pp. 851–872, 2019.

[38] Y. Arya, 'AGC performance enrichment of multi-source hydrothermal gas power systems using new optimized FOFPID controller and redox flow batteries," Energy., vol. 127, pp. 704–715, 2017.

[39] W. Tasnin, L. C. Siakia, "Impact of renewables and FACT device on deregulated thermal system having sine cosine algorithm optimised fractional order cascade controller," IET Renewable Power Generation., no. 9, vol. 13, pp. 1420 – 1430, 2019.

[40] Y. Arya, "A new optimized fuzzy FOPI-FOPD controller for automatic generation control of electric power systems," J. Franklin Inst., no. 11, vol. 356, pp. 5611–5629, 2019.

[41] Y. Arya. "AGC of PV-thermal and hydro-thermal power systems using CES and a new multi-stage FPIDF-(1+PI) controller," Renewab Energy., vol. 134, pp. 796-806, 2019.

[42] Z. Bingul and O. Karahan, " Comparison of PID and FOPID controllers tuned by PSO and ABC algorithms for unstable and integrating systems with time delay," Optim Control Appl Meth., Vol. 39, PP. 1431-1450, 2018.

[43] D. Sain, S. K. Swain, A. Saha, S. K. Mishra and S. Chakraborty, " Real-Time Performance Analysis of FOI-PD Controller for Twin Rotor MIMO System," IETE Technical Review., 36:6, 547-567, 2019. DOI: 10.1080/02564602.2018.1528190.

[44] V. Rajinikanth, K. Latha, "I-PD Controller Tuning for Unstable System Using Bacterial Foraging Algorithm: A Study Based on Various Error Criterion", Applied Computational Intelligence and Soft Computing., vol. 2012. https://doi.org/10.1155/2012/329389.

[45] S. M. Nosratabadi, M. Bornapour, and M. A. Gharnai, "Grasshopper optimization algorithm for optimal load frequency control considering Predictive Functional Modified PID controller in restructured multi-resource multi-area power system with Redox Flow Battery units," *Control Engineering Practice.,* vol. 89, pp. 204-227, 2019.

[46] J. M. Abdullah and T. A. Rashid, "Fitness dependent optimizer: In-spired by the bee swarming reproductive process," IEEE ACCESS, Vol. abs/1904.05226, 2019.

[47] D. S. Abdul-Minaam, W. M. E. S. Al-Mutairi, M. A. Awad and W. H. El-Ashmawi, "An Adaptive Fitness-Dependent Optimizer for the One-Dimensional Bin Packing Problem," in IEEE Access, vol. 8, pp. 97959-97974, 2020, doi: 10.1109/ACCESS.2020.2985752.

[48] D. A. Muhammed, S. A. M. Saeed and T. A. Rashid, "Improved Fitness-Dependent Optimizer Algorithm," in IEEE Access, vol. 8, pp. 19074-19088, 2020, doi: 10.1109/ACCESS.2020.2968064.

AMIL DARAZ was born in Pakistan, in 1989. He received, the B.E. degree in Electronics Engineering from COMSATS University Islamabad, Pakistan in 2012, the M.S. degree in Power and Control Engineering from International Islamic University Islamabad (IIUI), Pakistan, and currently Ph.D. scholar in Electical Engineering from International Islamic University Islamabad (IIUI), Pakistan. His research interests include control systems, Power system operation and Control, optimization of solving nonlinear problems.

SUHEEL. A. MALIK received the B.E. degree in Electrical & Electronics from Bangalore University, Bangalore, India in 1997, the M.S. degree in Electronic Engineering from Muhammad Ali Jinnah University (MAJU), Pakistan, and Ph.D. in Electronic Engineering from International Islamic University Islamabad (IIUI), Pakistan. Since 2007 has been with IIUI, where he is currently serving as Chairman/Associate Professor of the Department of Electrical Engineering (DEE). His research interests include control systems, numerical investigation of nonlinear problems, and application of nature-inspired metaheuristic algorithms for solving nonlinear problems. He has authored more than 30 journal and conference publications. He is also the reviewer of some journals and has served as member/chair in some international conferences.

HAZLIE MOKHLIS (Senior Member, IEEE) received the B.Eng. and M.Eng.Sc. degrees in electrical engineering from the University of Malaya (UM), Malaysia, in 1999 and 2002, respectively, and the Ph.D. degree from The University of Manchester, Manchester, U.K., in 2009. He is currently a Professor with the Department of Electrical Engineering, University of Malaya (UM), and the Head of the UM Power and Energy system (UMPES) research. His research interests include fault location, distribution automation, power system protection, and renewable energy He is also a Chartered Engineer in the U.K. and a Professional Engineer in Malaysia.

IHSAN UL HAQ completed his PhD (Electronics and Information Engineering) in 2009 from BeiHang University, Beijing China. He competed his MS (Electronics) in 2004 from Quad-i-Azam University, Islamabad, Pakistan. He has been working as Associate Professor in Department of Electrical Engineering, Faculty of Engineering and Technology, International Islamic University, Islamabad, Pakistan, Islamabad. His research areas are Image Processing, Hyperspectrral Image Processing, Medical Image Processing, Signal Processing, deep learning and Meta-heuristic Techniques. He has supervised 6 PhD and 25 MS students. He has published 35 journal and 15 proceeding articles.

FARHAN ZAFAR was born in Pakistan, in 1975. He received, the M.Sc. degree from University of Sindh Jamshoro, Pakistan, in 1999, M.Sc. degree in Physics from University of Sindh Jamshoro, Pakistan, in 2006 and the M.S. degree in Electronic engineering from International Islamic University Islamabad (IIUI), Pakistan in 2013, where he is currently pursuing the Ph.D. degree in electrical engineering. His research interests include control systems, under actuated systems, optimization and application of nature-inspired metaheuristic algorithms for solving nonlinear problems.

NURULAFIQAH NADZIRAH MANSOR received the B.Eng. degree from Vanderbilt University, USA, in 2008, the M.Eng. degree in power system engineering from the University of Malaya (UM), Malaysia, in 2013, and the Ph.D. degree from The University of Manchester, U.K., in 2018. From 2008 to 2014, she was a Process Engineer with Texas Instruments (M) Sdn. Bhd. She is currently a Senior Lecturer with UM. Her research interests include distribution system modeling and optimization, distribution system planning and operation, the integration of renewable energy, and smart grids